

**ornl**

ORNL/TM-7852

**OAK  
RIDGE  
NATIONAL  
LABORATORY**

**UNION  
CARBIDE**

**Cycle and Performance Analysis  
of Absorption Heat Pumps for  
Waste Heat Utilization**

Horacio Perez-Blanco and Gershon Grossman

**OPERATED BY  
UNION CARBIDE CORPORATION  
FOR THE UNITED STATES  
DEPARTMENT OF ENERGY**

ORNL/TM-7852

Contract No. W-7405-eng-26

ENERGY DIVISION

**CYCLE AND PERFORMANCE ANALYSIS OF ABSORPTION HEAT PUMPS  
FOR WASTE HEAT UTILIZATION**

Horacio Perez-Blanco and Gershon Grossman

Date Published - September 1981

Prepared by the  
OAK RIDGE NATIONAL LABORATORY  
Oak Ridge, Tennessee 37830  
operated by  
UNION CARBIDE CORPORATION  
for the  
DEPARTMENT OF ENERGY

## CONTENTS

	Page
NOMENCLATURE .....	v
ABSTRACT .....	1
EXECUTIVE SUMMARY .....	1
1. INTRODUCTION .....	5
2. THE ABSORPTION HEAT PUMP CYCLE .....	9
2.1. One- and Two-Stage Cycles .....	11
2.2. Open and Closed Cycles .....	13
3. SYSTEM PERFORMANCE CRITERIA .....	19
4. WORKING FLUIDS SELECTION .....	21
5. ABSORBER/EVAPORATOR SYSTEM PERFORMANCE .....	23
6. DESORBER PERFORMANCE .....	29
6.1. Closed Desorber .....	29
6.2. Open Desorber .....	32
7. OVERALL CYCLE PERFORMANCE .....	39
8. CONCLUSIONS .....	45
APPENDIX: OPEN DESORBER PERFORMANCE CALCULATIONS .....	47
REFERENCES .....	49

## NOMENCLATURE

$C_H$  — high solution concentration in the system (%)

$C_L$  — low solution concentration in the system (%)

$c_p$  — specific heat of water (kJ/kg·°C)

COP — coefficient of performance (dimensionless)

$(COP)_{th}$  — thermal coefficient of performance, excluding parasitics (dimensionless)

$(COP)_{max}$  — maximum possible coefficient of performance

$\Delta H$  — amount of waste heat delivered to open desorber (kJ)

$h_j$  — enthalpy at point  $j$  in the cycle (kJ/kg)

$m_j$  — flow rate at point  $j$  in the cycle (kg/s)

$Q$  — useful heat gain of the temperature-boosted stream (kJ)

$\Delta T$  — approach temperature at the desorber outlet (°C)

$T_f$  — final temperature of the upgraded heat (°C)

$T_g$  — temperature of solution leaving the desorber (°C)

$T_i$  — temperature of the input waste heat (°C)

$T_j$  — temperature at point  $j$  in the cycle (°C)

$T_s$  — heat sink temperature (°C)

$W_j$  — air humidity at point  $j$  in the cycle [(kg H<sub>2</sub>O)/(kg air)]

$W_i$  — air humidity at the air-solution interface [(kg H<sub>2</sub>O)/(kg air)]

$\epsilon_a$  — heat exchanger effectiveness in absorber (dimensionless)

$\epsilon_c$  — heat exchanger effectiveness in desorber (dimensionless)

$\epsilon_d$  — heat exchanger effectiveness in condenser (dimensionless)

$\epsilon_H$  — mass exchange effectiveness in open desorber

$\epsilon_r$  — heat exchanger effectiveness in recuperator (dimensionless)

# CYCLE AND PERFORMANCE ANALYSIS OF ABSORPTION HEAT PUMPS FOR WASTE HEAT UTILIZATION

Horacio Perez-Blanco and Gershon Grossman

## ABSTRACT

This report describes a theoretical analysis of a double-stage absorption heat pump cycle, performed as the first step toward the construction of a laboratory working system. The heat pump is designed to upgrade low-temperature waste heat by boosting its temperature typically from 60°C (140°F) to 120°C (250°F). The heat, which may be available from a variety of sources, is thereby made useful for industrial and other applications. The system uses part of the low-temperature heat as its energy source and does not need outside power, except for running small auxiliary equipment.

The heat pump employs an absorber/evaporator combination in which some hot water from the heat source is evaporated and the vapor is absorbed in a concentrated absorbent solution. The heat of absorption serves to raise the temperature of the rest of the hot water stream. Two stages of the above system are used in series to provide the desired temperature boost. Both are served by one desorber which uses part of the waste heat to concentrate the solution. The study considers both open- and closed-cycle regeneration of the solution.

The report describes the operation of the system and defines its performance criteria. Results of a computer study show the variation in performance with different design variables. Two working materials, LiBr-water and LiCl-water, are considered. The effect of different operating conditions is evaluated.

---

## EXECUTIVE SUMMARY

The U.S. industrial sector rejects annually about  $2.85 \times 10^6$  TJ of heat in the form of condensate, cooling water, and process water (at temperatures between 40 and 80°C), which amounts to roughly 3% of the U.S. annual energy consumption. Despite the low thermodynamic availability of this reject heat, its large amount justifies studying means for its recovery. To this end, and particularly for use as process heat, it is often necessary to upgrade its temperature. Absorption heat pumps offer an attractive alternative for this application because they rely on the waste heat itself as their source of power and do not require a primary energy source or mechanical work for their operation (except for parasitics, which may be kept small).

The purpose of the present study has been to explore the potential of absorption cycles for recovering waste heat at low temperatures [60°C (140°F)], as a first step toward the construction of a working system. Performance criteria have been defined in terms of parameters relevant to the operation of a low-grade-heat-actuated cycle. Several cycle configurations have been considered, including the use of different working materials. Component and system performances have been calculated.

The principle of the absorption heat pump is based on the physical phenomenon that when an absorbent solution is in vapor pressure equilibrium with a pure absorbed substance, the former has a higher temperature than the latter. The heat pump employs an absorber/evaporator combination in which some hot water from the low-grade-heat source is evaporated, and the vapor is absorbed in a concentrated absorbent solution.

The heat of absorption is produced at a temperature higher than that of the original warm water, according to the above principle. This heat serves to raise the temperature of the rest of the warm water stream. Two stages of the above system are used in series to provide the desired temperature boost. Both stages are served by one desorber which receives the diluted solution from the absorbers and uses additional waste heat to reconcentrate it. A more detailed description of the cycle is given in Chap. 2.

Two main performance criteria characterize the absorption heat pump: the temperature boost which the system can deliver and the coefficient of performance (COP). The latter is defined as the ratio of the heat delivered at the upgraded temperature to the energy input, which includes waste heat and parasitic power. The thermal COP (without parasitics) has a theoretical limit for given heat source and heat sink temperatures. This limit is set by the second law of thermodynamics. For example, for waste heat at 60°C (140°F), a reject heat temperature of 27°C (81°F), and a temperature boost of 50°C (90°F), the theoretical limit for the COP is 0.46. In the absorption heat pump, a higher temperature boost is traded off against a lower COP. Note that even if the waste heat is free, a low thermal COP is undesirable because it increases the amount of waste heat that must be handled by the system, thereby increasing initial cost and parasitic power. If the user is paying for disposal of the waste heat, however, the COP has a different economic meaning.

The criteria for selecting working fluids are discussed in detail in Chap. 4. Of the many possible material combinations, two were identified as promising candidates for the present type of heat pump: lithium bromide-water (LiBr-water) and lithium chloride-water (LiCl-water). The component and system analyses in this study were performed for these two working materials.

A component evaluation for the heat pump has been performed in the present study at the conceptual design level. The absorber/evaporator unit is the part of the heat pump where the temperature boost is produced. For preselected low and high solution concentrations and for a given wastewater flow rate and temperature, the performance of this unit increases with the heat exchange effectiveness. It depends also on the selection of the evaporation temperature. In a two-stage heat pump, the evaporation temperatures in the two stages can be selected independently. Both have a higher limit, which, when approached, results in very high water circulation rates. It is therefore desirable to select those two temperatures as high as possible, yet low enough below their limit for the flow rates in the system to be practical.

The desorber, often referred to as the generator, is the part of the heat pump responsible for concentrating the absorbent solution before it is brought into the absorber. The desorber performance and, in particular, the high solution concentration which it can produce depend on the heat supply temperature and on the heat rejection environment as manifested by the vapor pressure against which desorption takes place. The most desirable cycle configuration involves a closed desorber coupled with a condenser. The flow rates of hot supply water and cooling water to this system for given concentrations depend on the temperatures of those fluids, as well as on the heat exchange effectivenesses in the desorber and condenser. The higher the heat supply temperature and the lower the cooling water temperature, the better the performance and the lower the required flow rates. When cooling water is not available, or when its temperature is too close to that of the waste heat, an open desorber may be employed which uses the ambient air as a sink for the desorbed vapor. There, the specific humidity of the air is the controlling factor in performance instead of the cooling water temperature in a closed system.

The overall performance of the heat pump system is determined by its design characteristics as well as by the operating conditions. Design factors include primarily the heat exchange effectivenesses in the different components—the higher they are, the better the performance. Operating conditions include the waste heat and cooling water temperatures. The higher the waste heat temperature and the lower the cooling

water temperature, the better the performance. For given values of those temperatures, a higher COP may be obtained at the cost of a lower temperature boost by increasing the difference between the high and low solution concentrations.

The overall conclusion of the present study is that absorption cycles offer a good opportunity to recover waste heat at temperatures as low as 60°C (140°F). The study has yielded quantitative results for operating conditions and conceptual design parameters. The development of closed-cycle machines calls for a technology similar to that of conventional absorption chillers. Open-cycle desorbers, which may be required where sufficiently cold cooling water is unavailable, are a step further in terms of development needs. One typical result of using a two-stage heat pump of the preferred configuration described in this report, having a heat exchanger effectiveness of 0.85, is a temperature boost of 55°C (131°F) at a thermal COP of 0.36 with waste heat at 60°C (140°F) and cooling water at 15°C (59°F). At these temperatures, the corresponding Carnot COP is 0.53.

## 1. INTRODUCTION

The U.S. industrial sector consumes annually about  $3 \times 10^7$  TJ of primary energy [1] for heat and power. It has been estimated [2] that 50% of this energy is rejected to the environment as waste heat. This heat may be classified according to temperature [2]: high-temperature range, above  $650^\circ\text{C}$ ; medium-temperature range, between  $650$  and  $230^\circ\text{C}$ ; and low-temperature range, below  $230^\circ\text{C}$ . In the low range, a large part of the energy rejected is at temperatures below  $80^\circ\text{C}$ . In fact, the energy rejected in the form of condensate, cooling water, and process water (at temperatures between  $40$  and  $80^\circ\text{C}$ ) amounts to  $2.85 \times 10^6$  TJ/year [3], or roughly 3% of the U.S. annual energy consumption.

The amount of this heat that can be recovered is essentially determined by economics. Even though the thermodynamic availability of this reject heat is low, its large amount justifies studying means of recovering it for useful purposes. This heat may be used directly for space heating or for preheating process streams, among other applications [2]. In many instances, the temperature of the waste heat may not be high enough for its intended use. For example, Fig. 1 displays a profile of process heat consumption in different industrial sectors for the temperature ranges between  $60$  to  $100^\circ\text{C}$ ,  $100$  to  $140^\circ\text{C}$ , and  $140$  to  $180^\circ\text{C}$ . From this figure, it is evident that in order to use the low-temperature streams for process heat, it is desirable to upgrade their temperature. Heat pumps may be used for this purpose [3].

Vapor compression heat pumps, which require mechanical work for their operation, have been the most commonly suggested method for upgrading waste heat. Descriptions of vapor compression heat pumps and analyses of their potential for energy conservation may be found in [2] and [4]. Chiogioji [2] describes a conventional vapor compression system consisting of a condenser, an evaporator, a refrigerator compressor, and an expansion valve. These heat pumps are identified as useful devices for low-temperature waste heat recovery, typically for waste heat temperatures below  $121^\circ\text{C}$  and a typical COP ranging from 2 to 4, depending on the source and delivery temperatures. In [3], five heat pump types and applications are described. Electric power drives the compressor in three of them (liquid-to-liquid, air-to-air, and combined refrigeration-and-heating heat recovery applications). Vapor compression heat pumps driven by internal combustion engines and an advanced type driven by a gas turbine are also covered. Absorption heat pumps seem more attractive for use in upgrading waste heat, because they rely on the waste heat itself as their source of power and do not require mechanical work for their operation (except for parasitics, which may be kept small).

The fundamentals of temperature-boosting absorption are described, for instance, in [5]. Two alternative cycles are found most frequently in the literature [6]. In one of them, (Fig. 2a), high-temperature heat supply and low-temperature heat to be upgraded are the inputs to the heat pump, the useful output being at an intermediate temperature between the two [4, 6, 7]. The main application of these cycles takes place when a high-temperature source such as the combustion of natural gas is available. Gas-fired absorption heat pumps are probably the most common in this application [8]. In the other cycle, the heat input is all at the low temperature  $T_i$ . A fraction of it is upgraded to a temperature  $T_f$  greater than the input (Fig. 2b), whereas the remaining fraction is rejected to a sink at a temperature  $T_s$  lower than the input. Since

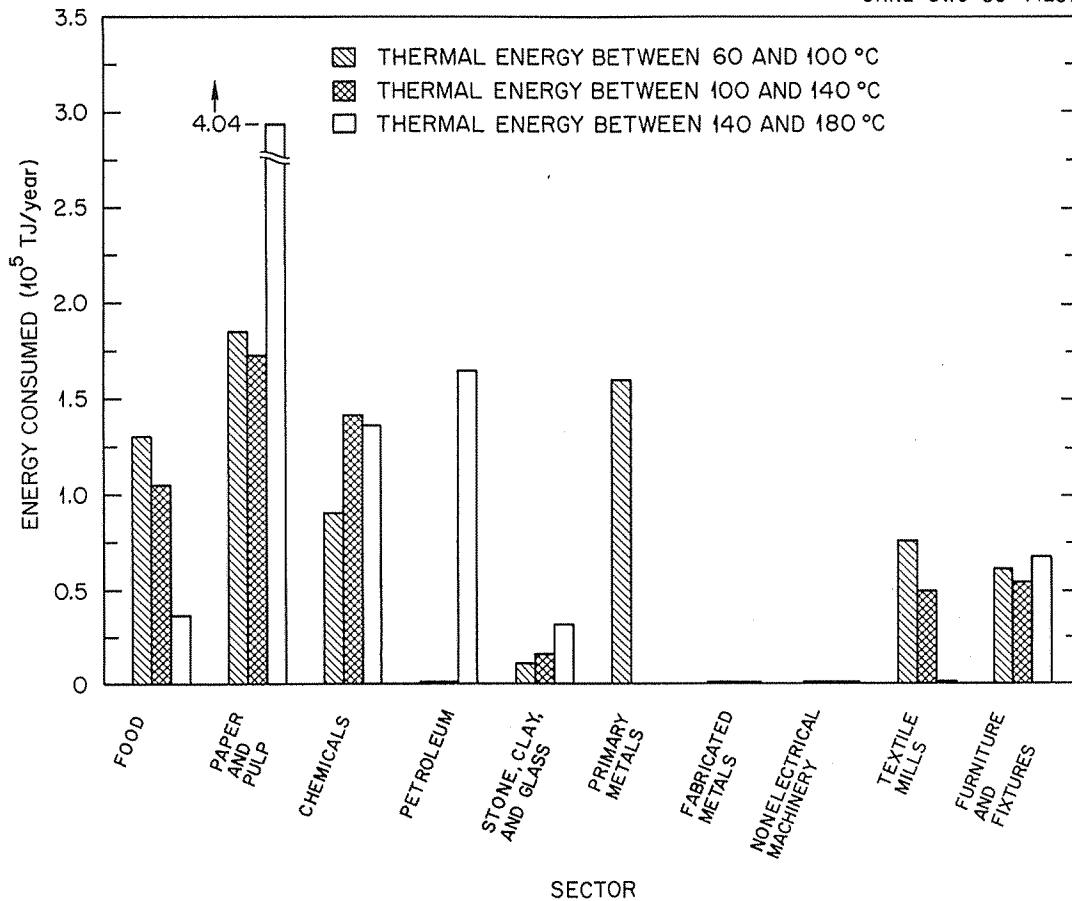


Fig. 1. Thermal energy consumed by different industrial sectors at different temperature levels.

this cycle does not call for high-grade heat for its operation, it is specially suited for working with low-temperature waste heat or with low-temperature solar energy [6]. It is known as a waste-heat-actuated cycle.

Several waste-heat-actuated cycles for providing industrial heat have been implemented with ammonia-water solutions. A one-stage absorption heat pump, operating on 65°C hot water, 15°C sink, and 105°C output temperatures, has been reported in the literature [9], even though details of construction and operation were not disclosed. An absorption-resorption heat pump developed at the French Institute of Petroleum (named the IFP Thermosorb Process) has also been described [10]. In this system, high efficiencies are possible for modest temperature boosts (about 30°C) at heat input temperatures above 70°C. For waste heat temperatures below 70°C, it was found that efficiencies drop substantially. A thermodynamic analysis of a two-stage, open-cycle LiBr-water absorption heat pump was presented in [11]. This analysis showed that large temperature boosts (from 60 to 105°C) are possible at 25% efficiencies, provided that the cycle operates at high solution concentrations. The potential of absorption-desorption systems has also been studied for providing space heating [6, 7, 12-15]. These applications generally call for lower delivery temperatures than do industrial applications and will not be described here.

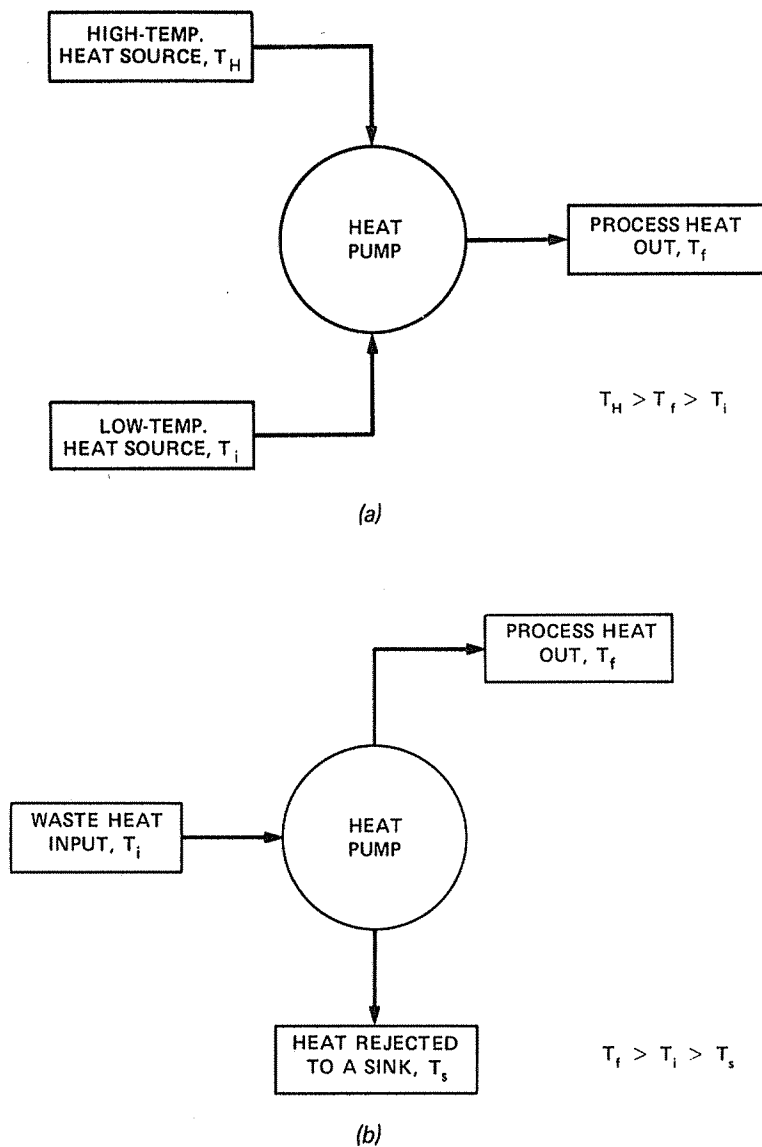


Fig. 2. Block diagram representation of heat pump cycles: (a) high-temperature heat-actuated; (b) waste-heat-actuated.

The purpose of the present study has been to explore the potential of absorption cycles for recovering waste heat at low temperatures ( $60^\circ\text{C}$ ) in order to provide process heat, as a first step toward the construction of a working system. Cycles that operate as illustrated in Fig. 2b are considered with LiCl-water and LiBr-water solutions as working fluids. The benefits of multistaging for achieving large temperature boosts are shown, and the merits of open-cycles for those applications where cooling water is not readily available are discussed. Performance criteria are defined by means of parameters that are relevant to the operation of a waste-heat-activated cycle. Components and overall system performance of a two-stage heat pump are calculated and the results discussed.

## 2. THE ABSORPTION HEAT PUMP CYCLE

Several versions of the absorption heat pump cycle may be used to achieve different degrees of temperature boosting under various operating conditions. In this chapter, the basic principles of operation of absorption cycles are presented. The need for multistaging to achieve larger temperature boosts for the assumed conditions is discussed. Open and closed cycles with their relative advantages and disadvantages are also described.

To illustrate the principle of the cycle, a schematic of a simple, one-stage, closed-cycle absorption heat pump is shown in Fig. 3. The state points defined in this figure\* are indicated on a LiBr-water property

ORNL-DWG 80-14249R4

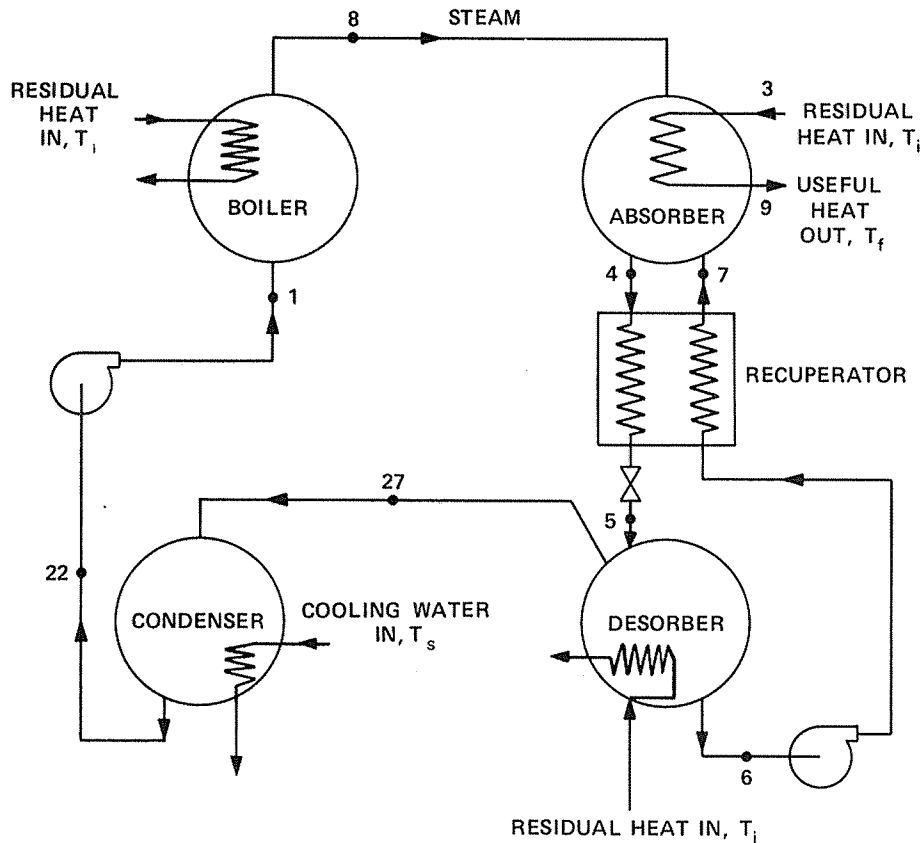


Fig. 3. Schematic of a single-stage absorption heat pump.

\*A state point numbering system is used consistently throughout the heat pump diagrams in this report. The numbers in later diagrams will correspond to those in Fig. 3.

diagram in Fig. 4. In this cycle, steam is generated in a boiler (pts. 1 to 8) by applying waste heat at temperature  $T_i$  as a heat source. The steam is absorbed in the absorber by a concentrated LiBr-water solution, releasing useful heat at a temperature higher than  $T_i$  (pts. 7 to 4). This heat is transferred to a water stream and boosts its temperature from  $T_i$  to  $T_f$ . The diluted solution (pt. 4) is cooled in a recuperative heat exchanger, and its pressure is reduced before entering the desorber (pts. 4 to 5). In the desorber, the solution is reconcentrated by evaporating water from it through the application of more waste heat at temperature  $T_i$ . The solution leaves the desorber (pt. 6), its pressure is raised by a pump, and it returns to the absorber via the recuperative heat exchanger (pts. 6 to 7). The steam leaving the desorber is condensed (pts. 27 to 22) and its pressure raised by a pump before entering the boiler (pt. 1).

ORNL-DWG 80-20813

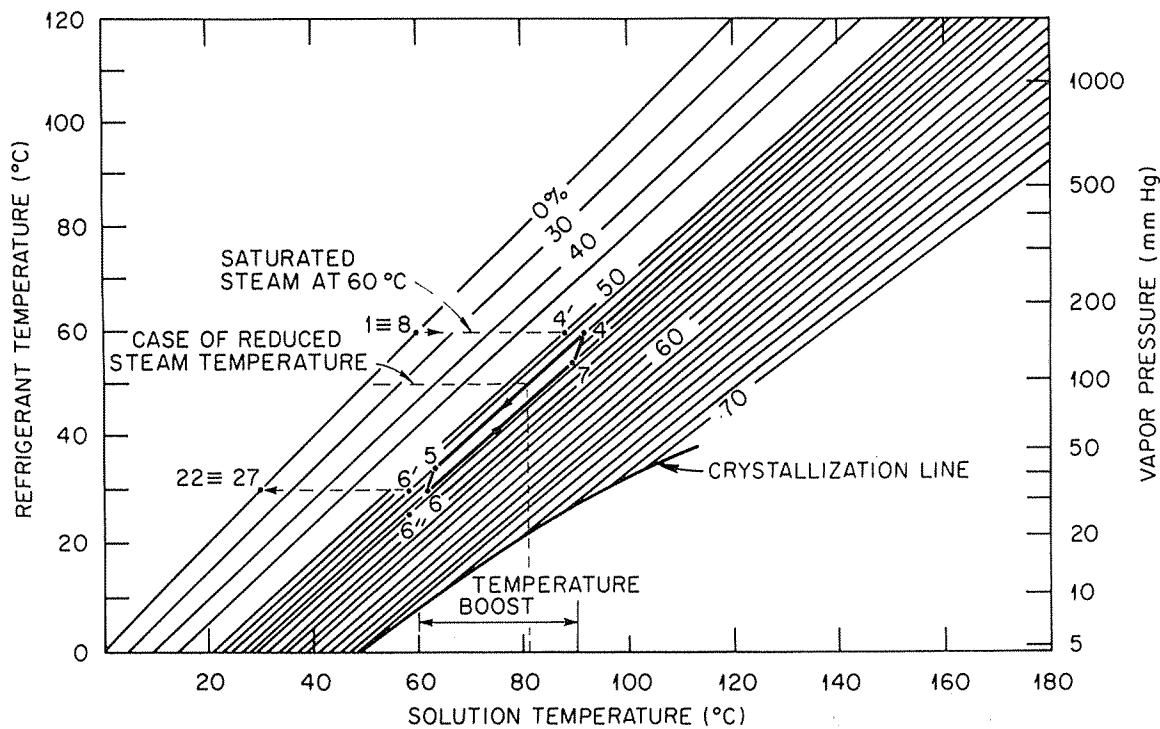


Fig. 4. Property diagram for a LiBr-water solution; the state points correspond to the heat pump cycle of Fig. 3.

Figure 4 describes a typical thermodynamic equilibrium diagram for the working fluid in the absorption heat pump. (The particular material combination shown here is LiBr-water.) The diagram describes the vapor pressure of pure water and the corresponding saturation temperature as a function of the LiBr-water solution temperature in equilibrium with it, for different solution concentrations. For a given concentration, the rise in vapor saturation temperature with the solution temperature is almost linear. Both are proportional to the logarithm of the vapor pressure. For a given solution temperature, the higher the concentration, the lower the equilibrium vapor pressure. Conversely, for a given vapor pressure or saturation temperature, the higher the concentration—the higher the solution temperature. The cycle points of Fig. 3 are indicated on the diagram.

The thermodynamic diagram of Fig. 4 illustrates the quantitative effects of the factors influencing the magnitude of the temperature boost. Clearly, it is desirable to have solution concentrations that are as large as possible. These are determined partly by the waste heat temperature  $T_i$ , which should ideally be as high as possible, and partly by the heat sink temperature  $T_s$ , which should be as low as possible. Once the concentrations have been fixed, the next important factor is the temperature of the steam generated in the boiler, which is a function of  $T_i$ .

It is clear from the above description that the heat pump operates between two pressures. The same low pressure prevails in the condenser and the desorber, and the same higher pressure in the boiler and absorber. In an actual design, the boiler and absorber would often be packaged in one high-pressure shell, and the desorber and condenser in a low-pressure shell, as illustrated in Fig. 5.

## 2.1 One- and Two-Stage Cycles

Generally, the temperature boosts needed for industrial applications are too large to be achieved in one stage. In the example described above (Fig. 4), if saturated steam at  $60^\circ\text{C}$  can be obtained from the waste heat and the desorption step proceeds also at  $60^\circ\text{C}$  with condensation at  $30^\circ\text{C}$ , temperature boosts in the order of  $30^\circ\text{C}$  may be obtained with high and low LiBr-water solution concentrations of 54% and 52%, respectively.

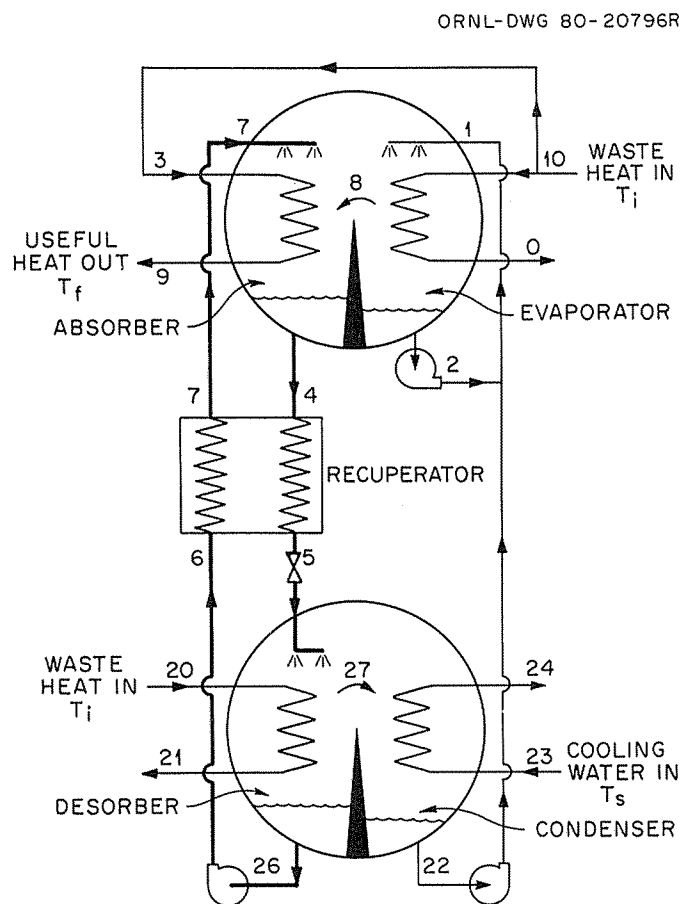


Fig. 5. Schematic of a single-stage absorption heat pump with main components enclosed in two separate shells.

Larger temperature boosts may be achieved by means of a two-stage cycle, as illustrated in Fig. 6. In this cycle, the condensate (pt. 1) enters the first-stage evaporator, where some of it is evaporated by means of waste heat (pts. 1 to 2). The steam produced (pt. 8) is absorbed by a LiBr solution, releasing heat (pts. 7 to 4). The dilute solution (pt. 4) returns to the desorber via a recuperative heat exchanger.

The heat released in this first stage is used to heat water (pts. 3 to 9), which is then divided into two fractions. One circulates in the second-stage evaporator where it releases heat to evaporate more condensate (pts. 11 to 12). The other fraction is heated further in the second-stage absorber by the heat of absorption

ORNL-DWG 80-20797R

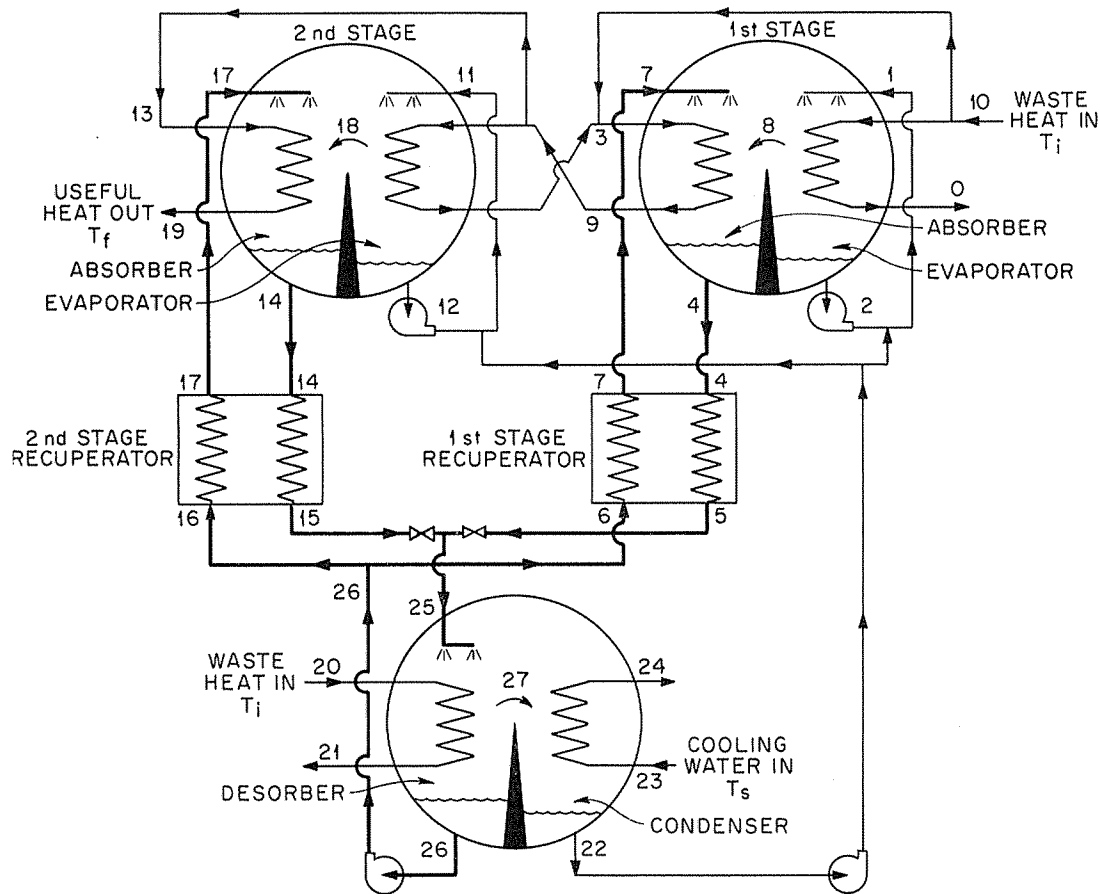


Fig. 6. Schematic representation of a two-stage closed absorption heat pump.

(pts. 13 to 19) and released as hot process water. The weak solution from the second stage (pt. 14) is returned to the desorber via a recuperative heat exchanger. In the desorber, the solution is concentrated using waste heat as a heat source (pts. 25 to 26). The evaporated water is condensed (pt. 22) and sent back to the evaporators, and the strong solution is pumped back to the absorbers via the recuperative heat exchangers.

The state points corresponding to Fig. 6 are shown on a LiBr-water equilibrium diagram in Fig. 7 for high and low solution concentrations of 54% and 52%, respectively. It is assumed that steam at 60°C is available from the waste heat, and that the solution temperature at the desorber outlet is also 60°C. For

the purpose of illustration of the increased temperature boost effect, a steam temperature of 83°C was assumed in the second-stage absorber. Temperature boosts in the order of 50°C may be obtained with the two-stage cycle.

The two-stage cycle described in Fig. 6 is a preferred configuration out of several other multistage concepts, which could be used to produce similar temperature boosts. One other possibility is to have the first stage in the configuration described in Fig. 5 and use the temperature-boosted stream out of the first-stage absorber as a heat source for a second desorber. This desorber would then be able to produce a more concentrated solution than the first one powered by the original waste heat. The more concentrated solution could be used in a second-stage absorber to give a high temperature boost [3]. In comparison with the preferred configuration of Fig. 6, this concept has several disadvantages. A detailed discussion of the various multistage concepts is beyond the scope of this report.

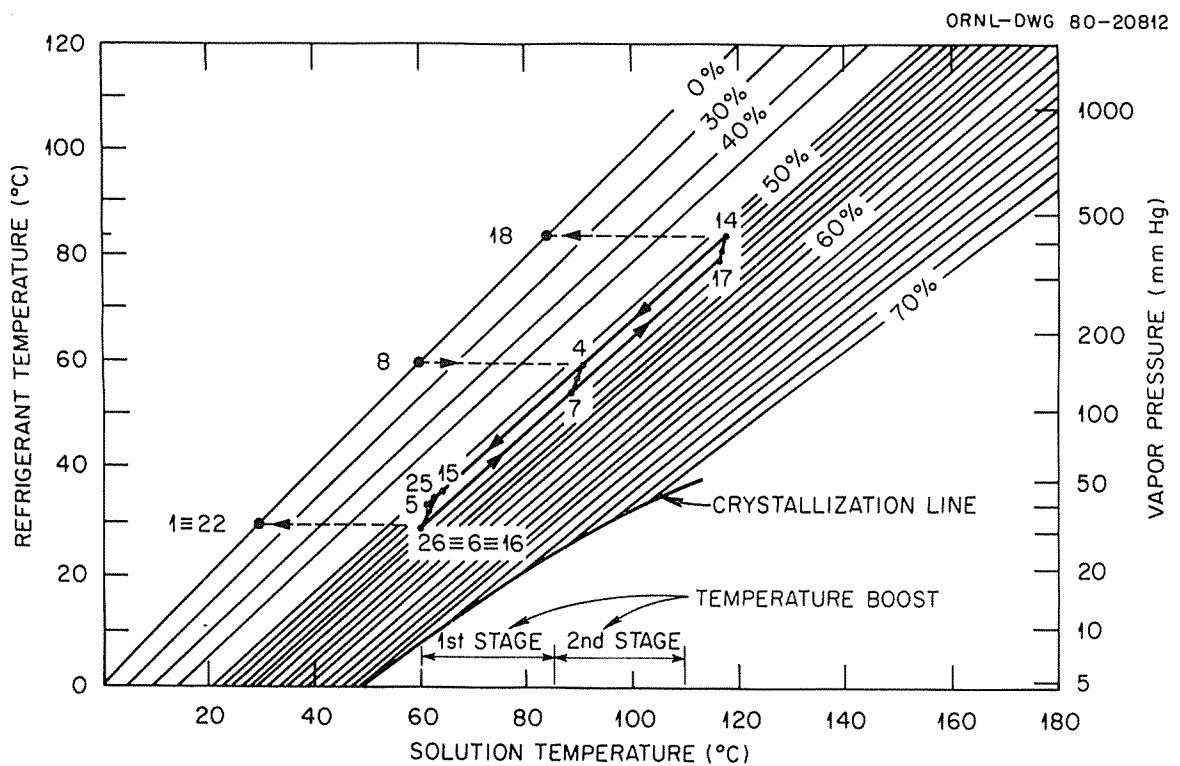


Fig. 7. Property diagram for a LiBr-water solution; state points correspond to the two-stage cycle of Fig. 6.

## 2.2 Open and Closed Cycles

In the examples described above, the maximum solution temperature in the desorber and the steam temperature in the evaporator were assumed equal to the waste heat temperature. In a real situation, a temperature drop is needed across heat exchangers in order to ensure good heat transfer. This temperature drop may seriously affect the cycle performance.

To illustrate, let us assume that hot waste water is available at a temperature of 60°C. When this water is used as a heat source in the boiler of the cycle illustrated in Fig. 3 for producing steam, a temperature difference between the minimum water temperature and the steam temperature must exist to induce good

heat transfer. Thus, if the water leaves the boiler at  $54^{\circ}\text{C}$  and a temperature drop of  $4^{\circ}\text{C}$  is assumed, then steam at only  $50^{\circ}\text{C}$  may be generated. The temperature boosting effect of the cycle is thus reduced from  $31^{\circ}\text{C}$  to approximately  $18^{\circ}\text{C}$ , as indicated in Fig. 4.

If instead of a closed evaporator as in Fig. 5, a flash chamber is employed (Fig. 8), a closer thermal equilibrium between the steam and the water leaving the chamber may be obtained. If the water is flashed from  $60$  to  $54^{\circ}\text{C}$ , a mass of steam at point 8 equal to 1% of the water mass would be produced. Thus, the

ORNL-DWG 80-20798R2

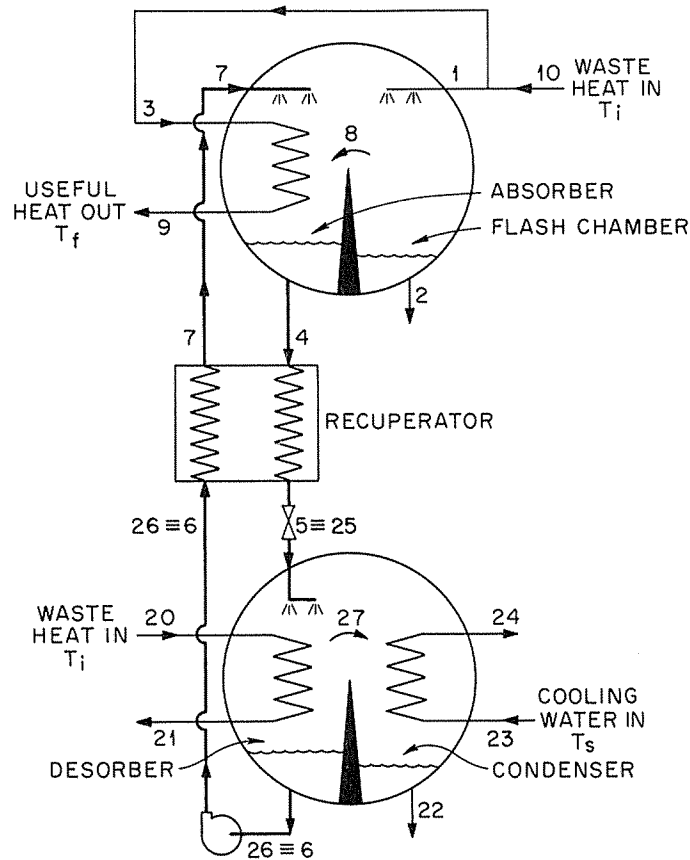


Fig. 8. Schematic of a single-stage absorption heat pump with a flash chamber instead of a closed evaporator.

water leaves the flash chamber and the closed evaporators at the same temperature ( $54^{\circ}\text{C}$ ), but the steam temperature is  $54^{\circ}\text{C}$  in the former and only  $50^{\circ}\text{C}$  in the latter. The temperature boost possible with a flash chamber is, therefore, larger than the one possible with a closed evaporator. In a flash chamber, the following advantages are realized over a closed evaporator:

1. a closer thermal equilibrium exists between the steam produced and the outgoing water;
2. there is an enhancement of the temperature-boosting effect; and
3. metallic heat exchanger surfaces are unnecessary.

The principal drawback of a flash chamber with a small temperature drop is the need to provide both large interfacial areas for evaporation and long liquid residence times. This may produce a somewhat



For example, if the condensation temperature was reduced from 30 to 25°C, conserving the maximum solution temperature of 57°C, then point 6' would be displaced to 6", and the maximum cycle concentration would be 55%. Reducing the condensation temperature is equivalent to reducing the vapor pressure in the condenser, from 31 mm Hg to 24 mm Hg. When cooling water at a low enough temperature is not available, the solution water may be directly evaporated into atmospheric air [16, 17] whose water vapor pressure may be as low as 18 mm Hg in hot, humid summer days (32.2°C dry bulb and 29°C wet bulb).

The concept of open desorption thus offers the following advantages over closed desorption:

1. a lower waste heat temperature may be used when cold enough cooling water is not available;
2. no cooling water is needed, and, therefore, cooling tower equipment, piping, and parasitic power are eliminated; only makeup water to replace what has evaporated into the air is needed; and
3. no condensing surfaces are needed, which eliminates the metallic area of the condenser and also eliminates its auxiliaries (controls, pumps, purges, etc.).

This concept has two main drawbacks:

1. As the solution exchanges mass with the air, heat is also transferred to it. To preserve high levels of thermal efficiency, it may be necessary to install an air-to-air heat recuperator. This device may recover both the sensible and part of the latent heat transferred to the air, but it will increase capital costs and parasitic power necessary to handle large air volumes.
2. Exposing a LiCl- or LiBr-water solution to the air causes oxygen and dust impurities to dissolve into the solution. This may cause corrosion problems, which call for the use of corrosion-resistant materials and/or corrosion inhibitors.

The heat pump cycle with an open desorber may take on different configurations, as indicated in Sects. 2.1 and 2.2. A cycle with flash evaporators and an open desorber may be implemented as illustrated in Fig. 9. The steam entering the device in the flash chambers is evaporated into a stream of air after serving its useful purpose. The state points for this cycle are similar to those indicated in Fig. 7. If cooling water at low enough temperatures is available, it is possible to combine the two-stage flash chambers with a closed desorber/condenser, as shown in Fig. 10. In this case, the condensed water is simply disposed of, or it may be reheated in order to restart the cycle.

In this report we will focus on a two-stage cycle with flash evaporators, coupled with either a closed or an open desorber. As outlined above, the largest temperature boosts may be obtained with these configurations. The wastewater temperature will be taken equal to 60°C in all cases, and other relevant parameters will be varied to calculate performance under different conditions.

STATE POINT	TEMPERATURE		FLOW (kg/s)
	°F	°C	
1	140.0	60.0	10.7
2	129.8	54.3	10.6
3	172.9	78.3	6.6
4	191.8	88.8	2.3
5	144.3	62.4	2.3
6	131.0	55.0	2.2
7	182.7	83.7	2.2
8	129.8	54.3	0.1
9	189.0	87.2	6.6
10	140.0	60.0	1.1
11	189.0	87.2	5.64
12	179.1	81.8	5.58
13	189.0	87.2	1.0
14	247.8	119.9	1.2
15	156.8	69.3	1.2
16	131.0	55.0	1.1
17	230.3	110.1	1.1
18	179.1	81.7	0.06
19	239.0	115.0	1.0
20	140.0	60.0	20.5
21	132.4	55.8	20.5
22	68.0	20.0	0.2
23	59.0	15.0	23.3
24	66.7	19.3	23.3
25	148.6	64.8	3.4
26	131.0	55.0	3.3
27	139.8	60.0	0.2

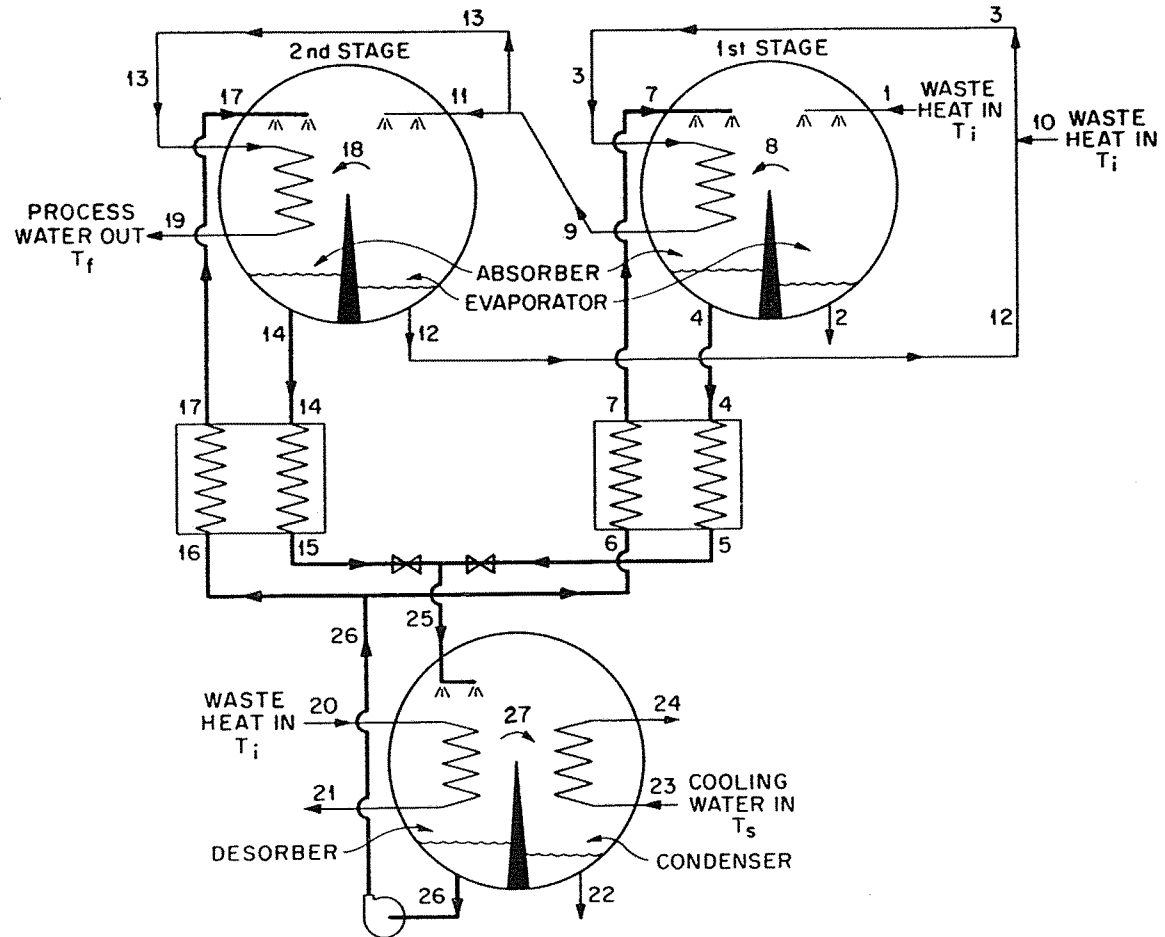


Fig. 10. Schematic of a two-stage, closed-desorber heat pump. Table shows the temperatures and flow rates at all state points under typical operating conditions as obtained from the computer code described in Sects. 3-5.

### 3. SYSTEM PERFORMANCE CRITERIA

The performance of the absorption heat pump is characterized by several parameters that should be considered in the design of an efficient working system. These performance parameters depend on two given operating conditions: the temperature of the source of heat to be upgraded ( $T_i$ ) and the heat rejection environment as determined by the cooling water or ambient air, whichever is applicable. For the latter condition, the characteristic parameter is the vapor pressure of the evaporating fluid against which desorption must take place. In a closed system, this is determined by the condensing temperature which in turn depends on the cooling medium; in an open system, it is determined by the absolute humidity of the air. For these two given conditions, the design variables of the system, such as the absorbent concentrations and different flow rates, must be selected so as to optimize the performance parameters.

The first and perhaps most important performance characteristic of the heat pump is the output temperature ( $T_f$ ) which the system can deliver with given heat source and heat rejection temperatures. Clearly, a large temperature boost is desirable. However, for each cycle configuration with given working materials and number of stages,  $T_f$  has a theoretical upper limit, as will be shown in the next sections. Trying to operate close to this limit results in very large heat exchange surfaces and high flow rates. The latter are associated with excessive pumping power requirements. A practical choice of  $T_f$  must consider these factors.

Another important performance criterion is the overall coefficient of performance (COP) of the system, defined as the ratio between the useful heat output and the energy input. The latter consists of two parts: input from the heat source and parasitic power. In systems where the second part is negligibly small, the overall COP is essentially equal to the thermal COP. Using the notation of Figs. 8-10,  $(COP)_{th}$  is given by

$$(COP)_{th} = \frac{m_{19}(T_f - T_i)}{m_2(T_i - T_2) + m_{21}(T_i - T_{21}) + m_{22}(T_i - T_{22})} \quad (1)$$

In this equation,  $T$  stands for the temperature and  $m$  for the mass flow rate at the point indicated. For comparison, it would be of interest to calculate the COP of the same operating conditions with the ideal Carnot cycle. Assuming a reversible heat engine operating in place of the desorber/condenser between two heat reservoirs at temperatures  $T_i$  and  $T_s$  and supplying work to a reversible heat pump operating in place of the absorber/evaporator between two heat reservoirs at  $T_f$  and  $T_i$ , the following expression is obtained:

$$(COP)_{max} = \frac{T_f(T_i - T_s)}{T_i(T_f - T_s)} \quad (2)$$

For typical conditions  $T_i = 333$  K ( $60^\circ\text{C}$ ),  $T_f = 383$  K ( $110^\circ\text{C}$ ), and  $T_s = 300$  K ( $27^\circ\text{C}$ ), the maximum COP that results from Eq. (2) is 46%.

The parasitic power consumers in the system include circulation pumps, air fans, purge systems, etc. At given operating temperatures, the power required is usually proportional to the third power of the amount of

fluids circulated. Increasing these flows can often help raise the thermal COP at the cost of increasing the parasitic power requirements.

A key consideration in the design of the heat pump system is the price of the heat to be upgraded. If this heat is taken as being abundantly available and free, the system should be designed to minimize the parasitic power requirements (possibly resulting in a low thermal COP). For example, waste heat not only is free but often entails an additional cost to dispose of. With a source of heat such as solar or geothermal, however, the thermal COP is of greater importance.

The last, but not least, performance criterion of the system is its initial cost. As in many similar cases, good thermal performance calls for the temperature differentials in the heat exchangers to be kept to a minimum. The designer must weigh this consideration against the cost of the heat exchangers, which are a major part of the overall system's cost.

#### 4. WORKING FLUIDS SELECTION

The properties required of absorbent/refrigerant combinations for use in absorption cooling systems have been discussed extensively in the literature [18–20]. Many of these requirements are equally applicable to a heat pump system of the type discussed in the present report. The most important characteristics may be summarized as follows: (1) The equilibrium temperature of the absorbent/refrigerant solution in equilibrium with the vapor should be as high as possible at the absorber conditions and as low as possible at the desorber conditions. This requirement provides for a maximum temperature boost and ease of regeneration. (2) The solubility of the refrigerant in the absorbent must be as high as possible at the absorber temperature and pressure and as low as possible at the corresponding desorber conditions. In other words, the concentration difference between the strong and weak absorbent, as determined by the conditions in the desorber and absorber, respectively, should be as large as possible. If this requirement is not met, large amounts of absorbent solution must be circulated between the absorber and desorber in order to transfer the necessary quantity of refrigerant, thus causing excessive internal heat losses. (3) The heat of absorption/desorption should be as high as possible at the absorber conditions and as low as possible at the desorber conditions. This heat is the sum of the latent heat of vaporization/condensation of the refrigerant and of the heat of dilution. The latter should therefore be as high as possible in the absorber and as low as possible in the desorber to enhance the COP. (4) The properties of the absorbent/refrigerant solution, which affect heat and mass transfer (such as viscosity, diffusion coefficient, thermal conductivity, etc.), should be favorable. (5) The absorbent should be nonvolatile, or considerably less volatile than the refrigerant, to prevent the transfer of absorbent into the condenser or regenerating air. A nonvolatile absorbent is an absolute must in open systems. (6) The saturation concentration of the absorbent/refrigerant solution should be as high as possible and beyond the range of operating concentrations of the system at the given temperature. (7) The working fluids should be chemically stable, nonflammable, nontoxic, noncorrosive to common materials of construction, and available at a reasonable cost.

Of the many fluid pairs considered and experimented with for absorption systems, only a few were found practical, having satisfied most of the above criteria. Water-ammonia and LiBr-water have been used extensively in closed-cycle cooling systems, each with its own merits and disadvantages. In the former pair, ammonia is toxic and the absorbent (water) is volatile, requiring a rectifier between the desorber and condenser. The LiBr-water combination is corrosive to metals and the salt crystallizes out of solution at high concentrations. These problems have been dealt with effectively in closed-cycle cooling systems, and both fluid pairs seem suitable for absorption heat pumps. The LiBr-water pair is clearly more promising because, in the water-ammonia combination, the working pressures are high even in cooling applications and become much higher at the heat pump range of working temperatures—to the point where construction may become impractical. Other working fluid combinations have been tested in experimental closed-cycle absorption setups [20], but it appears that none has shown a definite advantage justifying its use in place of the first two.

Open-cycle absorption cooling systems have invariably employed water as the refrigerant, with various absorbents including lithium bromide, lithium chloride, calcium chloride, ethylene glycol, and several types of solid absorbents of water [21]. Again, of the many candidate materials, two emerge as being most suitable for the heat pump system. These are the LiBr and LiCl absorbents, both nonvolatile and satisfying

most of the above criteria. Another possible absorbent is calcium chloride, which, although inferior to LiBr and LiCl, is less expensive and less corrosive than the lithium salts.

The present study considers LiBr-water and LiCl-water as working materials for the heat pump system, both in the closed- and open-cycle configurations. The intention is not to rule out other combinations but rather to evaluate the potential of the cycle with what seem to be the most suitable fluid pairs at present. Figures 4 and 7 show a typical equilibrium diagram for the LiBr-water combination, based on data from over 15 sources compiled recently by McNeely [22]. Similar data for LiCl-water have been provided [23, 24]. Enthalpy data were also obtained from those references.

In selecting the operating concentrations for the system, several points must be taken into consideration. With a given working fluid pair, it is desirable to operate at the highest possible concentrations in the absorber, thus achieving a large temperature boost. The limit on the high concentration is set by the conditions in the desorber, as determined by the heat source temperature and by the vapor pressure. Better results may be achieved with higher heat source temperatures and with lower vapor pressures, as brought about by low-temperature cooling water or low-humidity air. Once the high concentration is determined, the low concentration may be selected close to it for a high temperature boost; on the other hand, the larger the concentration difference, the lower the availability losses associated with the solution circulation in the system. A larger temperature boost is, hence, traded off against a lower COP.

## 5. ABSORBER/EVAPORATOR SYSTEM PERFORMANCE

The part of the heat pump in which the actual temperature boosting takes place is the absorber/evaporator system. Under the configuration discussed in the present report (see Figs. 9 and 10), it consists of two stages, both served by the same desorber. In this chapter, the performance of this system is analyzed, and the considerations leading to its optimization are reviewed.

The basic unit of the absorber/evaporator system in a multistage absorption heat pump is described in Fig. 11. A notation consistent with the one for the overall system (Figs. 9 and 10) is used to mark the different points in the cycle. The unit consists of an absorber and a flash chamber used for an evaporator,

ORNL-DWG 80-20803R2

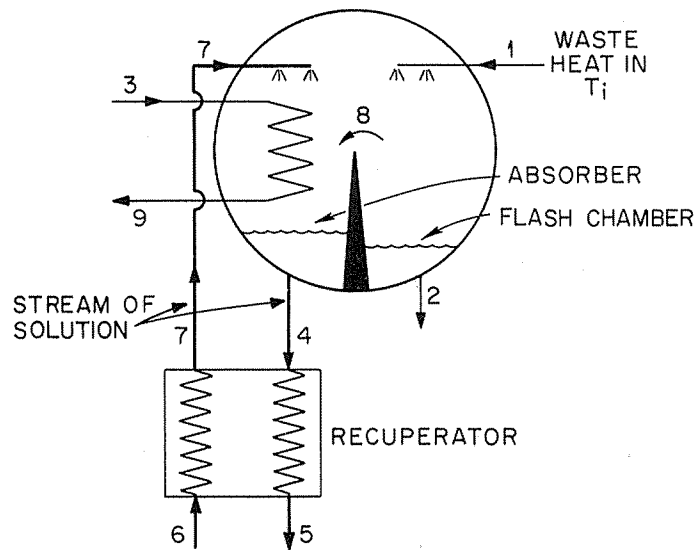


Fig. 11. Schematic of the absorber/flash chamber subsystem, also showing the recuperator.

both packaged in the same shell. Water entering the flash chamber at state 1 is evaporated in part and leaves at a somewhat lower temperature at state 2. The vapor (state 8) is absorbed in the stream of solution entering at state 7 and leaving at 4. The heat of absorption serves to boost the temperature of the water stream entering at 3 and leaving at 9. A recuperative heat exchanger is also part of this basic unit, transferring heat from the weak to the strong solution.

In the following analysis, the high and low absorbent concentrations ( $C_H$  and  $C_L$ , respectively) are preselected. The former is determined by the conditions in the desorber; the latter is a variable for performance optimization, the effect of which will be evaluated and discussed. The temperature of the strong solution entering the recuperator (state 6) is also fixed by the desorber and will be referred to as  $T_g$ . The properties of all other states may be calculated as functions of the above parameters and of the temperature

of the heat source to be upgraded ( $T_i$ ). Heat exchanger effectivenesses  $\epsilon_a$  and  $\epsilon_r$  are assumed for the absorber and recuperative heat exchanger, respectively. The effectiveness is defined as the ratio of the actual heat transferred to the thermodynamically limited, maximum possible heat transfer rate [25]. Two basic assumptions are made: (1) the weak solution leaving the absorber (state 4) is in vapor pressure equilibrium with the vapor coming from the evaporator (state 8), and (2) pressure drops in the system are negligible.

For the given concentrations and temperatures, the following equations may be written to describe the process in the absorber/evaporator system:

1. in the evaporator:

$$\text{mass balance: } m_8 = m_1 - m_2 , \quad (3)$$

$$\text{energy balance: } m_8 h_8 = m_1 c_p T_1 - m_2 c_p T_2 , \quad (4)$$

$$T_2 = T_8 ; \quad (5)$$

2. in the absorber:

$$\text{equilibrium: } T_4 = f(T_8, C_L) , \quad (6)$$

$$\text{salt mass conservation: } m_4 C_L = m_7 C_H , \quad (7)$$

$$\text{mass balance: } m_8 = m_4 - m_7 , \quad (8)$$

$$\text{energy balance: } m_3 c_p (T_9 - T_3) = m_7 h_7 + m_8 h_8 - m_4 h_4 , \quad (9)$$

$$m_3 = m_9 , \quad (10)$$

$$\text{absorber effectiveness: } \epsilon_a = (T_9 - T_3)/(T_4 - T_3) ; \quad (11)$$

in the recuperator:

$$m_4 = m_5 , \quad (12)$$

$$m_6 = m_7 , \quad (13)$$

$$\text{recuperator effectiveness: } \epsilon_r = (T_7 - T_6)/(T_4 - T_6) , \quad (14)$$

$$\text{heat balance: } m_4h_4 - m_5h_5 = m_7h_7 - m_6h_6 . \quad (15)$$

Here,  $m$ ,  $h$ , and  $T$  indicate the mass flow rate, enthalpy, and temperature of the working material at the different states, respectively, and  $c_p$  is the specific heat of water.

The enthalpies of the solution at the different states may be expressed in terms of the temperature and concentration;  $h_8$  is the enthalpy of dry saturated steam at temperature  $T_8$ . With the inlet flow rates  $m_1$  and  $m_3$  and inlet temperatures  $T_1$ ,  $T_3$ , and  $T_6$  given, the above set of equations may be solved for the temperatures and flow rates at all nine states.

By combining Eqs. (7), (8), and (9), an expression may be obtained for the heat gain of the temperature-boosted stream:

$$Q = m_3c_p(T_9 - T_3) = m_8[h_8 - (C_Hh_4 - C_Lh_7)/(C_H - C_L)] . \quad (16)$$

The term in square brackets indicates the amount of heat contributed toward a temperature boost per unit mass of vapor evaporated and absorbed. Of the enthalpy of that vapor ( $h_8$ ), a portion is subtracted to account for the loss of available heat due to the imperfect recuperative heat exchanger and the finite heat of dilution of the solution. It is clear from this term that the larger the concentration difference ( $C_H - C_L$ ), the larger the heat gain. With  $C_H$  determined by the conditions in the desorber, it seems desirable from this point of view to lower  $C_L$ . However, the temperature boost itself is given by

$$(T_9 - T_3) = \epsilon_a(T_4 - T_3) , \quad (11a)$$

and  $T_4$  is lower for lower  $C_L$ . This leads again to the conclusion stated on a qualitative basis in Chap. 4, that an optimum must be found for  $C_L$  by trading off a high temperature boost for a lower heat gain.

A system of equations similar to Eqs. (3)–(15) may be written for the second stage of the absorber/evaporator system.\* In combining the two stages, the following additional conditions are in effect:

$$T_{11} = T_9 , \quad (17)$$

$$T_{13} = T_9 , \quad (18)$$

$$m_{11} + m_{13} = m_9 , \quad (19)$$

$$m_3 = m_{10} + m_{12} , \quad (20)$$

$$m_3c_pT_3 = m_{10}c_pT_{10} + m_{12}c_pT_{12} . \quad (21)$$

---

\*The indices used to mark the different points in the second stage correspond to those of the first with 10 added to each. Thus, the entrance point of water to the evaporator is marked 1 in the first stage and 11 in the second stage; the evaporation temperature is 8 in

With the flow rate of the output stream  $m_{19}$  selected arbitrarily as a measure of size of the system and with the given inlet temperatures  $T_1 = T_{10} = T_i$ ,  $T_6 = T_{16} = T_g$ , there are altogether 36 equations for the 38 unknown temperatures and flow rates at points 1 through 19. Two of the latter can hence be selected as free parameters for optimization.

A computer program has been written to carry out the above calculation. In selecting  $m_{19}$  as unity, the temperature boost and the heat gain of the output stream are given by the same expression. It makes physical sense to select as the free optimization parameters the evaporation temperatures in the first and the second stages,  $T_8$  and  $T_{18}$ , respectively. These are also the saturation temperatures corresponding to the pressures prevailing in the two stages. Figure 12 shows an operating map of the absorber/evaporator system in terms of these parameters. The figure describes the temperature boost ( $T_f - T_i$ ) as a function of the mass ratio between the rejected and useful streams ( $m_2/m_{19}$ ). The working material is LiBr-water. The heat source temperature is fixed at  $T_i = 60^\circ\text{C}$  ( $140^\circ\text{F}$ ) and the solution from the desorber is at 54% and 57°C ( $134^\circ\text{F}$ ). Two sets of curves are shown for the low concentration at 50 and 52%.

It is clear from the operating map that the higher the evaporation temperature at both stages, the higher the temperature boost. For a given  $T_8$ , raising  $T_{18}$  results in a significant rise in temperature boost without

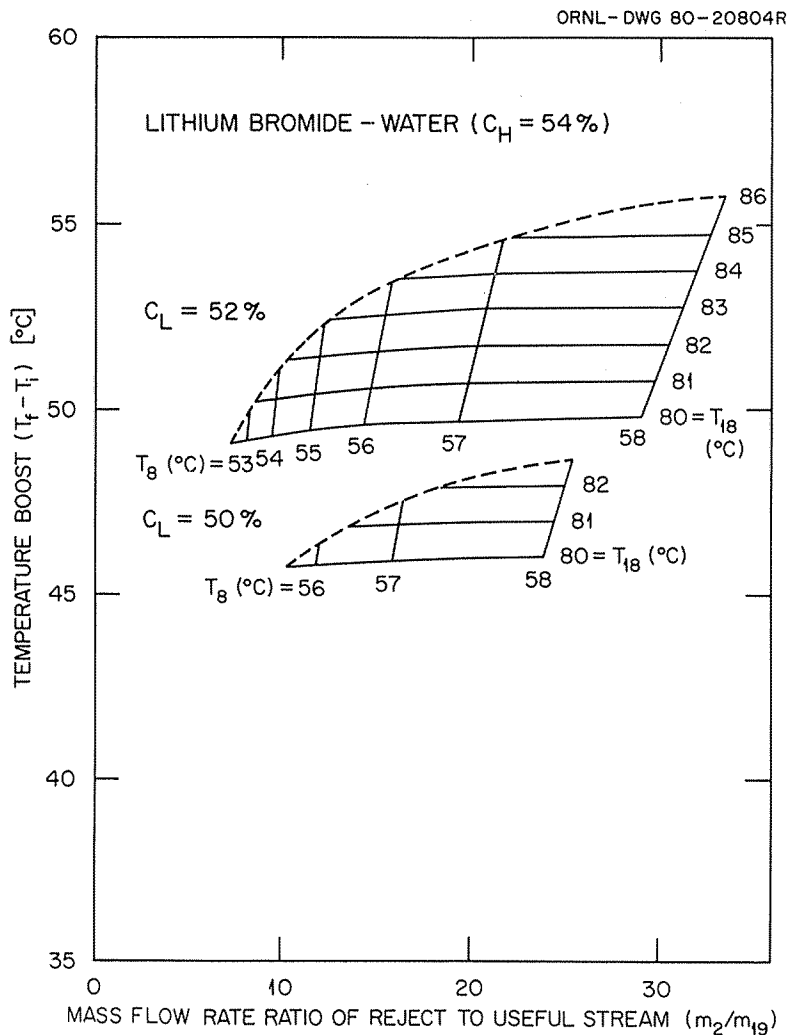


Fig. 12. Performance map for the absorber/flash chamber combination with a LiBr-water solution.

greatly increasing the mass of the rejected stream. The opposite is not as desirable: increasing  $T_8$  at fixed  $T_{18}$  only slightly raises the temperature boost and considerably increases the mass rejected.

While  $T_8$  and  $T_{18}$  can be selected independently, there is an upper limit on both. The upper limit for  $T_8$  is the heat source temperature  $T_i$ , and bringing the former close to the latter results in a rapid increase of the rejected stream  $m_2$ . For each  $T_8$ , the upper limit on  $T_{18}$  is set by the condition that the water temperature in both absorbers is always lower than that of the solution. Thus, the requirement of  $T_3 < T_7$  determines the maximum output temperature of the first stage as

$$T_9 < T_4 - (1 - \epsilon_{a1})(1 - \epsilon_{r1})(T_4 - T_8) , \quad (22)$$

where  $T_4 = T_4(T_8, C_L)$  in equilibrium. Equation (22) is obtained by combining Eqs. (11) and (13). The corresponding  $T_{18}$  and second-stage output temperature  $T_{19}$  are then determined by the rest of the system. When approaching this limit on  $T_{18}$ , the amount of water circulated between the first and second stage (e.g.,  $m_{12}$ ) becomes very large. All other operating parameters are reasonably practical. Therefore, a good choice would be to select  $T_8$  somewhat below  $T_i$  so as to have a reasonable  $m_2$  and then to select  $T_8$  somewhat below its limit corresponding to  $T_8$  so that  $m_{12}$  will not be too large.

The effect of the low concentration is also evident from Fig. 12. Lowering the concentration from 52 to 50% reduces the temperature boost by about 3.5°C, for the same values of  $T_8$  and  $T_{18}$ . It also reduces the maximum  $T_{18}$  attainable for each  $T_8$ . The rejected stream  $m_2$  is reduced somewhat, indicating a better heat gain of the upgraded stream under the lower  $C_L$ .

Figure 13 shows an operating map similar to that of Fig. 12, with LiCl-water as the working fluid. The high concentration of this solution has been selected at 41%, which has the same vapor pressure at 57°C as a 54% LiBr solution when leaving the desorber. Again, two sets of curves are shown for the low concentration at 39 and 37%. A comparison of Figs. 12 and 13 shows that the LiBr solution gives a larger temperature boost than the LiCl when desorbed under the same conditions.

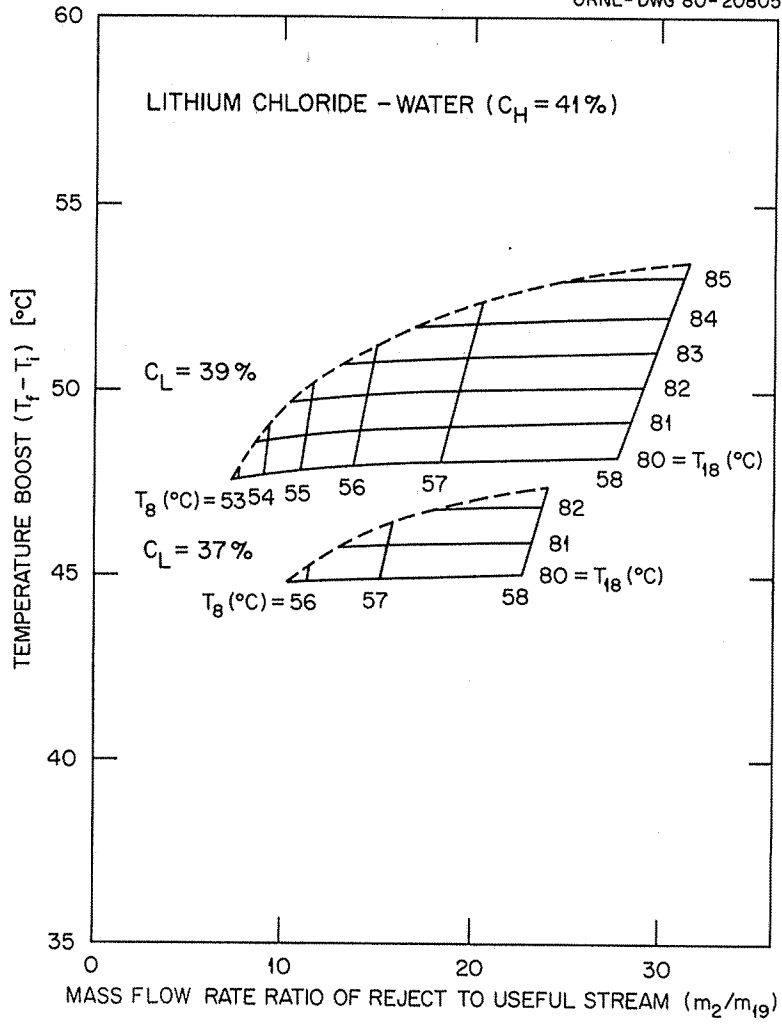


Fig. 13. Performance map for the absorber/flash chamber combination with a LiCl-water solution.

## 6. DESORBER PERFORMANCE

The desorber, often referred to as a generator, is the part of the heat pump system responsible for concentrating the absorbent solution before it returns to the absorber. The high solution concentration in the system is determined by the desorber, and the higher that concentration is, the higher the temperature boosting which may be achieved and the better the overall performance. In the present configuration of the system, both stages of the absorber/evaporator are served by one desorber. In some other configurations, the desorber may also be staged.

The performance of the desorber depends on the heat supply temperature and on the heat rejection environment as manifested by the vapor pressure and the corresponding saturation temperature. Ideally, the former temperature should be as high as possible and the latter as low as possible to achieve maximum concentration. In many conventional absorption units for which the heat supply temperature is not limited, a closed desorber is used in conjunction with a condenser. This is generally a good arrangement with many advantages. However, as explained in Chap. 2, when the heat supply temperature is low (as is often the case with low-grade heat) and when the ambient temperature is not sufficiently low to provide adequate cooling for the condenser, one would have to resort to an open desorber. In this chapter, both closed and open desorbers are analyzed.

### 6.1 Closed Desorber

Figure 14 describes schematically a closed-cycle desorber for the two-stage heat pump. Dilute solution at state 25, combining the dilute streams from both absorbers, enters the desorber and is heated by indirect contact with water entering at 20 and leaving at 21. Vapor at state 27 (normally somewhat superheated) is desorbed from the dilute solution and condenses, while the concentrated solution leaves at state 26. A condensing temperature (pt. 22) is provided by the cooling water entering the condenser at state 23 and leaving at 24.

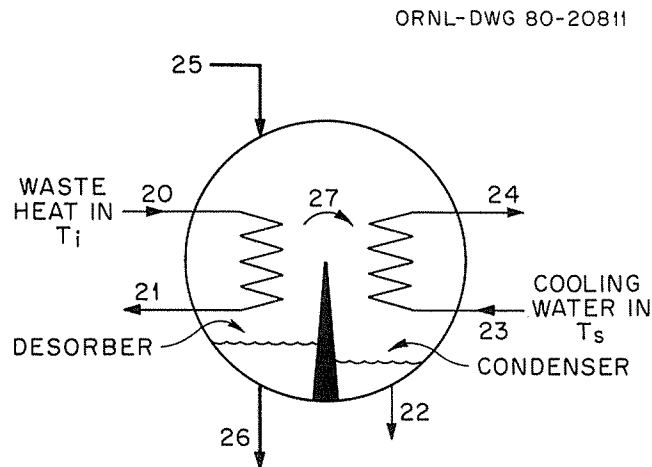


Fig. 14. Schematic of the closed desorber/condenser subsystem.

In the following analysis we will use the notation of Fig. 14 and assume heat exchanger effectivenesses  $\epsilon_d$  and  $\epsilon_c$  for the desorber and condenser, respectively. The following equations may be written to describe the process in the desorber/condenser system:

1. in the desorber:

$$\text{salt mass conservation: } m_{25}C_L = m_{26}C_H, \quad (23)$$

$$\text{mass balance: } m_{27} = m_{25} - m_{26}, \quad (24)$$

$$\text{energy balance: } m_{20}c_p(T_{20} - T_{21}) = m_{26}h_{26} + m_{27}h_{27} - m_{25}h_{25}, \quad (25)$$

$$m_{20} = m_{21}, \quad (26)$$

$$\text{equilibrium: } T_{26} = f(T_{22}, C_H), \quad (27)$$

$$\text{approximate desorbed vapor temperature: } T_{27} = (T_{25} + T_{26})/2, \quad (28)$$

$$\text{desorber effectiveness: } \epsilon_d = (T_{20} - T_{21})/(T_{20} - T_{26}); \quad (29)$$

2. in the condenser:

$$\text{mass balance: } m_{27} = m_{22}, \quad (30)$$

$$\text{energy balance: } m_{23}c_p(T_{24} - T_{23}) = m_{27}(h_{27} - h_{22}), \quad (31)$$

$$m_{23} = m_{24}, \quad (32)$$

$$\text{condenser effectiveness: } \epsilon_c = (T_{24} - T_{23})/(T_{22} - T_{23}). \quad (33)$$

The enthalpies of the solution at the different states may be expressed in terms of the temperature and concentration. By specifying the inlet conditions of the solution ( $m_{25}$ ,  $T_{25}$ , and  $C_L$ ), the high concentration required ( $C_H$ ), and the inlet hot and cooling water temperatures ( $T_{20}$  and  $T_{23}$ ), the above set of equations may be solved for the flow rates and temperatures of all eight states, with one free parameter for optimization. It makes physical sense to select as that parameter the condensing temperature  $T_{22}$ , as was done in the analysis of the absorber/evaporator system.

Figure 15 shows an operating map of the desorber with LiBr-water, obtained from a computer solution of Eqs. (23)–(33). The relative flow rates of hot water and cooling water are plotted for different cooling temperatures. [The waste heat temperature is fixed at 60°C (140°F)]. The inlet low concentration and required high concentration are 52 and 54%, respectively, and the effectiveness of both the desorber and

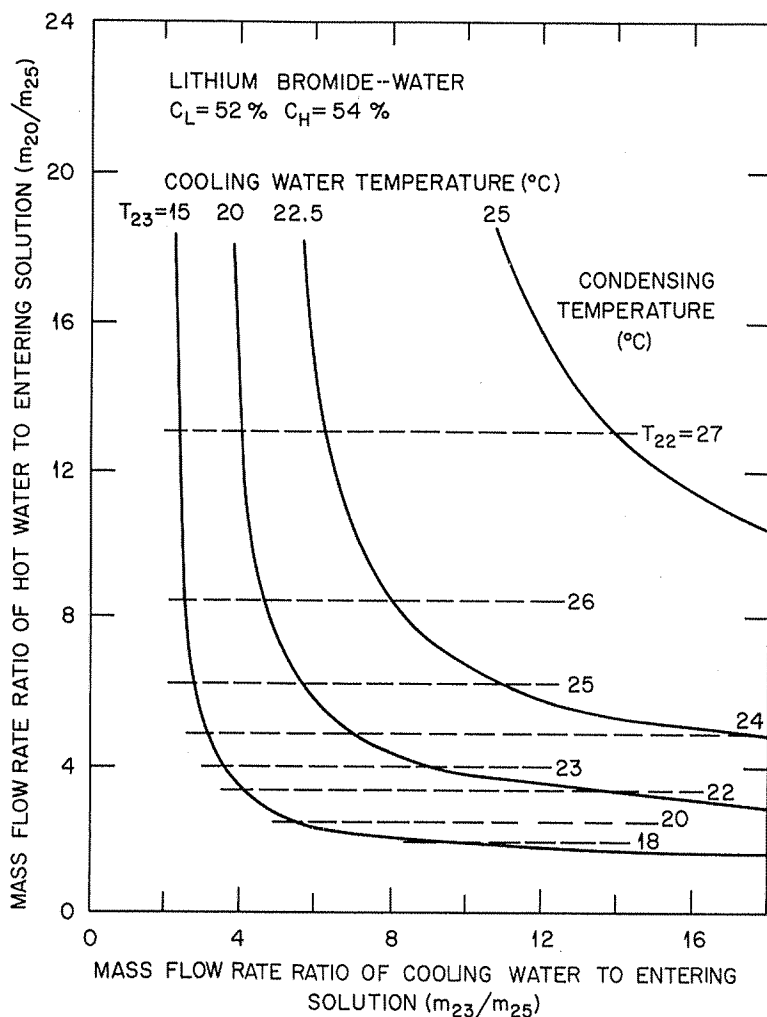


Fig. 15. Performance map for the desorber/condenser combination with a LiBr-water solution.

condenser is 0.80. It is clear from the figure that as the cooling water temperature increases, larger and larger flow rates of both cooling and hot water are required to produce the desired change in concentration. The upper limit on the condensing temperature is set by the required high concentration and the waste heat temperature available, through the equilibrium condition [Eq.(27)]. This limit may never be achieved in practice. Figure 15 also shows the hot water flow rate to be dependent directly on the condensing temperature  $T_{22}$  and to increase very rapidly as the limit on  $T_{22}$  is approached. The higher  $T_{22}$ , the smaller the amount of cooling water required.

An additional run of the computer program was made to obtain a similar operating map of the desorber for LiBr high and low concentrations of 54 and 50%, respectively. The results are very similar to those of Fig. 15 with the flows of hot water ( $m_{20}$ ) and cooling water ( $m_{23}$ ) per unit mass of entering solution ( $m_{25}$ ) approximately doubled. This is to be expected, since the amount of vapor desorbed is now about twice as large as in the previous case. The main conclusion is that the amounts of hot water and cooling water needed are a function of the amount of water desorbed, when the high concentration is fixed, except for additional second-order effects.

Figure 16 shows an operating map similar to that of Fig. 15 for a LiCl-water solution. Here again, as in the absorber/evaporator analysis, the high concentration of the solution has been selected at 41%, which yields the same vapor pressure at 57°C as LiBr at 54%. It is clear from Figs. 15 and 16 that for the same condensing temperature, larger quantities of both cooling and hot water are required to produce a 2% change in concentration in LiCl than are required for the LiBr. This is to be expected because the amount of water desorbed is higher in the case of LiCl, being 0.0488 kg per kilogram of entering solution as opposed to 0.0370 kg for LiBr. The ratio  $m_{20}/m_{23}$  remains about the same for both working materials.

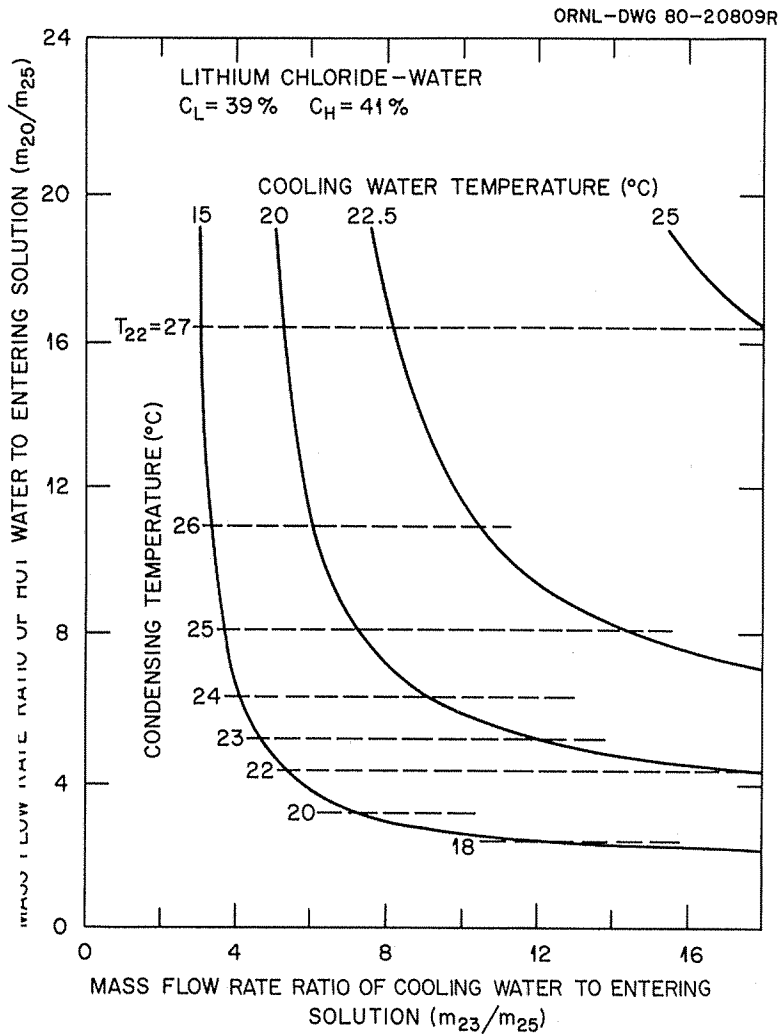


Fig. 16. Performance map for the desorber/evaporator combination with a LiCl-water solution.

## 6.2 Open Desorber

When an open desorber is used instead of a closed one, performance calculations become more involved because an open desorber involves a two-phase, three-component heat and mass transfer process. Performance analysis of an adiabatic open desorber and of an open desorber with heat addition are presented in

[16] and [17], respectively. In this report, desorber performance is calculated based on a simplified model. The objective of these calculations is to provide optimum design parameters.

In our simplified model (Fig. 17), the solution enters the desorber, where water evaporates from it in direct contact with the air, flowing countercurrent to the solution. Waste heat is added continuously to the solution to keep both its temperature and vapor pressure high so that evaporation can proceed. If waste heat were not added during this process, the solution temperature and vapor pressure would decrease rapidly

ORNL-DWG 80-20810R

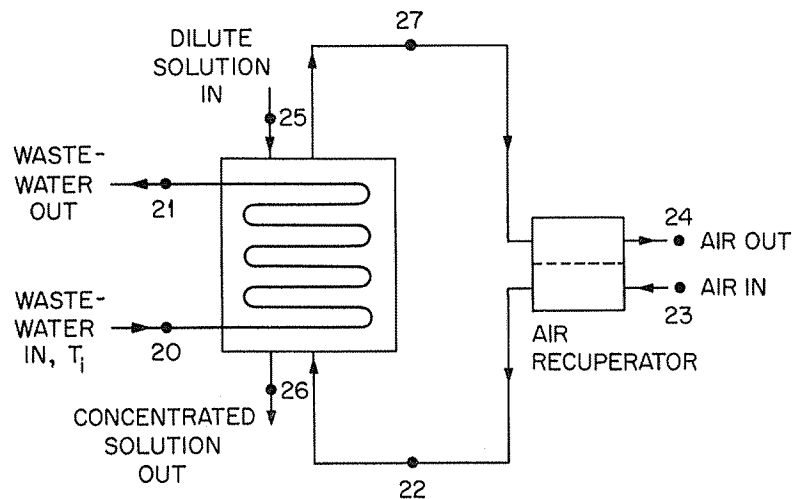


Fig. 17. Schematic of an open desorber/air-to-air recuperator subsystem.

until equilibrium with the air vapor pressure was reached. At this point, all mass exchange would cease. The situation, idealized in this model, may be achieved in practice in a packed tower with heat-exchanging coils immersed in the packing, or in a falling film evaporator with countercurrent flow of air.

To calculate performance, the following assumptions have been made:

1. The solution vapor pressure is maintained constant during desorption (pts. 25 to 26 in Fig. 17) by continuous addition of waste heat.
2. The resistance to mass transfer is concentrated in the air, and it is negligible in the solution.

An analysis of the simultaneous heat and mass transfer process in the air has been performed, the details of which are given in the appendix. By considering the analogy between the heat and the mass transfer in turbulent flow and by assuming a Lewis number close to unity, a relation has been derived between the air temperatures and humidities in the inlet and outlet bulk flow and at the air-solution interface.

The following equations may be written to describe the process in the open desorber system:

$$\text{salt mass conservation: } m_{25}C_L = m_{26}C_H, \quad (34)$$

$$\text{water mass balance: } m_{23}(W_{27} - W_{22})/(1 + W_{23}) = m_{25} - m_{26}, \quad (35)$$

$$\text{mass exchange effectiveness: } \epsilon_H = (W_{27} - W_{22})/(W_i - W_{22}) , \quad (36)$$

$$\text{solution exit temperature: } T_{26} = T_{20} - \Delta T , \quad (37)$$

$$\text{equilibrium conditions: } W_i = f(T_{26}, C_H) , \quad (38)$$

$$T_{25} = g(W_i, C_L) , \quad (39)$$

where  $\Delta T$  is the approach temperature at the desorber outlet,  $W$  designates air humidity, and  $W_i$  is the humidity at the air-solution interface.

From the Lewis analogy (see appendix for details):

$$(W_i - W_{22})/(W_i - W_{27}) = (T_{26} - T_{22})/(T_{26} - T_{27}) , \quad (40)$$

$$\text{air recuperator effectiveness: } T_{27} = T_{23} + (T_{22} - T_{23})/\epsilon_r , \quad (41)$$

$$\text{heat balance around recuperator: } T_{24} = T_{27} - T_{22} + T_{23} , \quad (42)$$

where  $\epsilon_r$  is the air-to-air heat recuperator effectiveness, and the changes in air heat capacity due to moisture pickup have been neglected. In addition,

$$\begin{aligned} \text{overall heat balance: } \Delta H &= m_{20}C_p(T_{20} - T_{21}) \\ &= m_{23}(h_{24} - h_{23})/(1 + W_{23}) + m_{26}h_{26} - m_{25}h_{25} , \end{aligned} \quad (43)$$

where the air enthalpies are given for 1 kg of dry air mass and  $\Delta H$  stands for the amount of waste heat delivered to the desorber. Finally,

$$\text{desorber heat exchange effectiveness: } \epsilon_d = (T_{20} - T_{21})/(T_{20} - T_{25}) . \quad (44)$$

In the equations listed above, the air and solution enthalpies can be calculated once the temperatures and concentrations of water are known. With conditions  $m_{23} = m_{22}$ ,  $m_{27} = m_{24}$ ,  $W_{27} = W_{24}$ ,  $m_{20} = m_{21}$ , and  $m_{23} = m_{22}$  (Fig. 17), the system presented above has 12 equations with 20 unknowns. If the approach temperature  $\Delta T$ , the high and low concentrations  $C_H$  and  $C_L$ , the initial air moisture  $W_{23}$  and temperature  $T_{23}$  and the initial water temperature  $T_{20}$  are specified, the number of unknowns is reduced to 14. Because no condensation takes place in the recuperator,  $W_{22}$  equals  $W_{23}$ . Then, by adopting  $m_{25}$ , the inlet solution mass flow rate, equal to one, it is possible to solve the above system for the 12 remaining unknowns.

Once the approach temperature  $\Delta T = T_{26} - T_{20}$  and the high concentration  $C_H$  are chosen, point 26 is determined (Fig. 4). The solution vapor pressure may be calculated from the diagram and  $W_i$  calculated. The air temperature and moisture changes may then be calculated, given the initial conditions  $T_{23}$  and  $W_{23}$ ,

and an overall heat balance produced to give  $\Delta H$ . The temperature of the entering solution  $T_{25}$  is assumed to be in equilibrium with the inlet concentration and vapor pressure. Calculations were carried out by means of a computer code of Eqs. (34) to (44).

The most critical variable in this method of calculation is the approach temperature  $\Delta T$  between the solution and the waste heat, since, together with the high concentration  $C_H$ , it determines the solution vapor pressure at the desorber outlet. A performance map of the desorber as a function of the approach temperature is shown in Fig. 18 with LiBr-water as the working fluid. Mass exchange effectiveness is 0.75, high and low concentrations are 54 and 52%, respectively, and the waste heat temperature is 60°C. In quadrant

ORNL-DWG 80-20814 R2

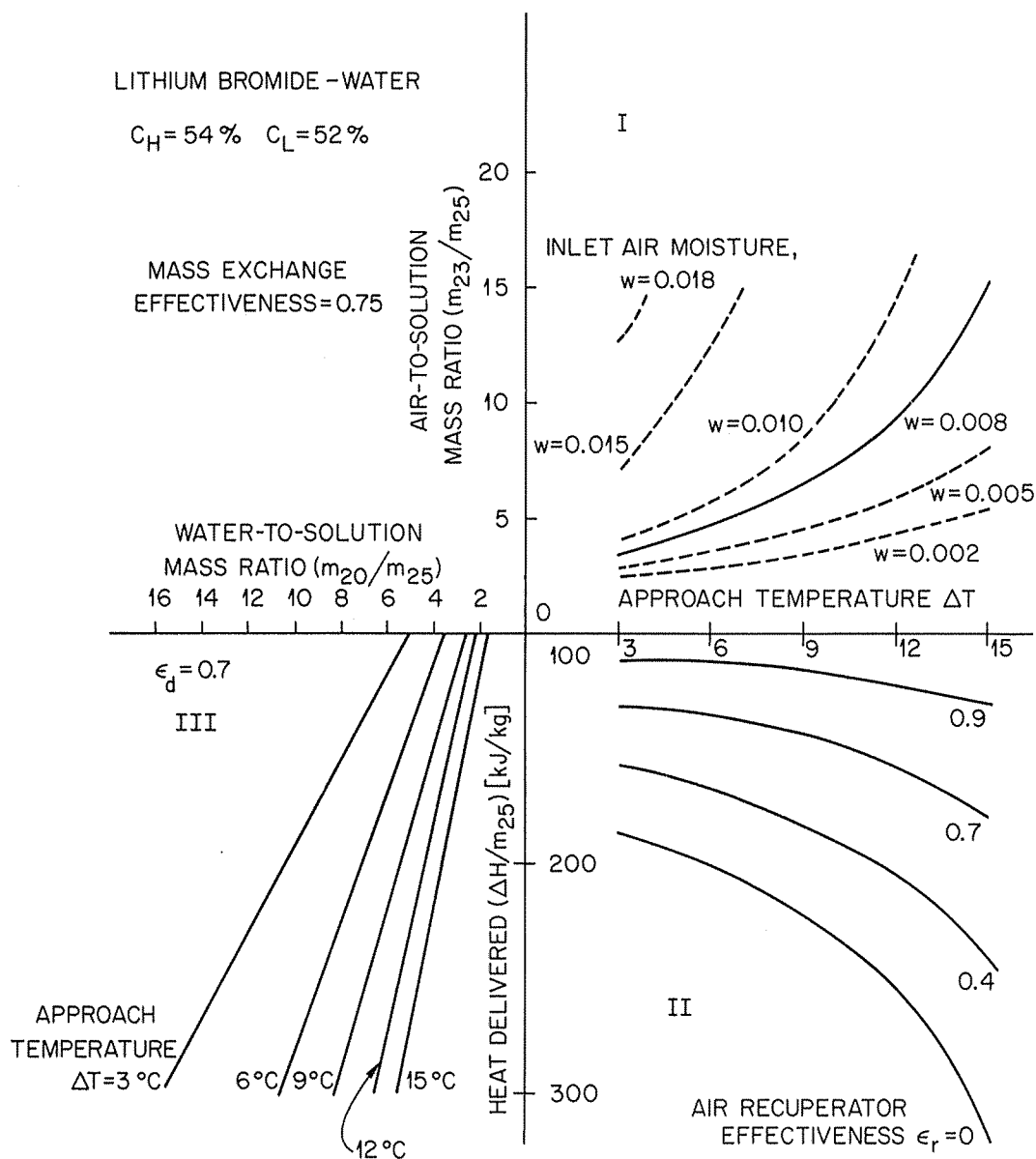


Fig. 18. Performance map for the open desorber/air-to-air recuperator subsystem with a LiBr-water solution.

## 7. OVERALL CYCLE PERFORMANCE

The performance of the individual components of the heat pump has been analyzed in the previous chapters. In this chapter, the overall system performance is studied. A computer program similar to those described in previous chapters was used to calculate the state points at different operating conditions and from them the performance parameters.

Figure 20 describes the temperature boost ( $T_f - T_i$ ) and the thermal COP [Eq. (1)] for the closed-cycle system (Fig. 10) as a function of the low concentration. The waste heat temperature is  $60^\circ\text{C}$  and the

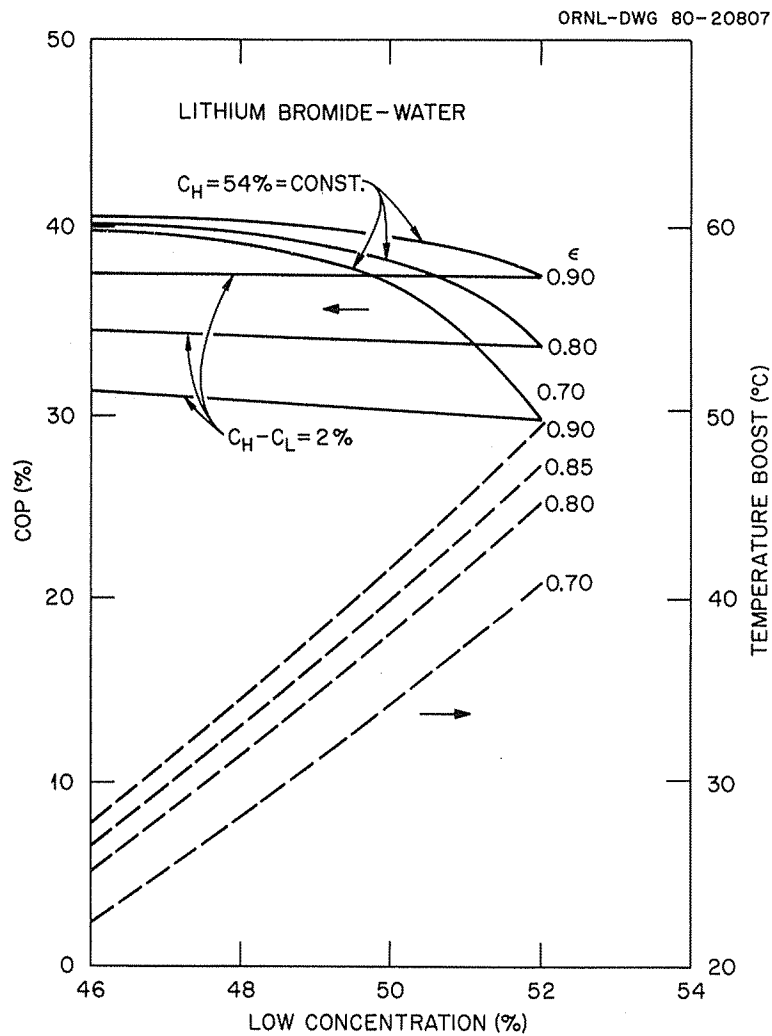


Fig. 20. Performance map showing the effect of concentration on COP and temperature boost for a LiBr-water solution for the two-stage absorption heat pump with a closed desorber.

condensing water temperature is maintained constant at 20°C. The working material is LiBr-water, and a series of curves are shown for different values of the heat exchanger effectiveness, assumed to be the same for all the heat exchangers in the system. Two sets of runs were made for each value of  $\epsilon$ : in one, the high concentration is fixed at 54%; in the other,  $C_H$  is higher than  $C_L$  by a constant 2%. As expected, the temperature boost is independent of  $C_H$  and determined primarily by the low concentration. The broken lines indicate the temperature boost to increase with  $C_L$  and, of course, with the heat exchanger effectiveness. The COP turns out to be sensitive to the concentration difference. With  $C_H - C_L = 2\%$ , the change of COP with the low concentration is very small. However, if  $C_H$  is kept constant, one can achieve a significant increase in COP by lowering  $C_L$ , at the expense of a reduced temperature boost. The change in COP is more significant for the system with low heat exchanger effectiveness. There the losses due to solution circulation are highest, and, therefore, a larger gain is achieved by increasing the concentration differences. Once this difference becomes large, on the order of 8%, the COP is about the same for all  $\epsilon$ 's.

Figure 21 shows a similar set of curves for LiCl-water. A behavior similar to that of the LiBr (Fig. 20) is observed. The high concentration of the solution is kept constant at 41% (The LiBr was kept at 54%.)

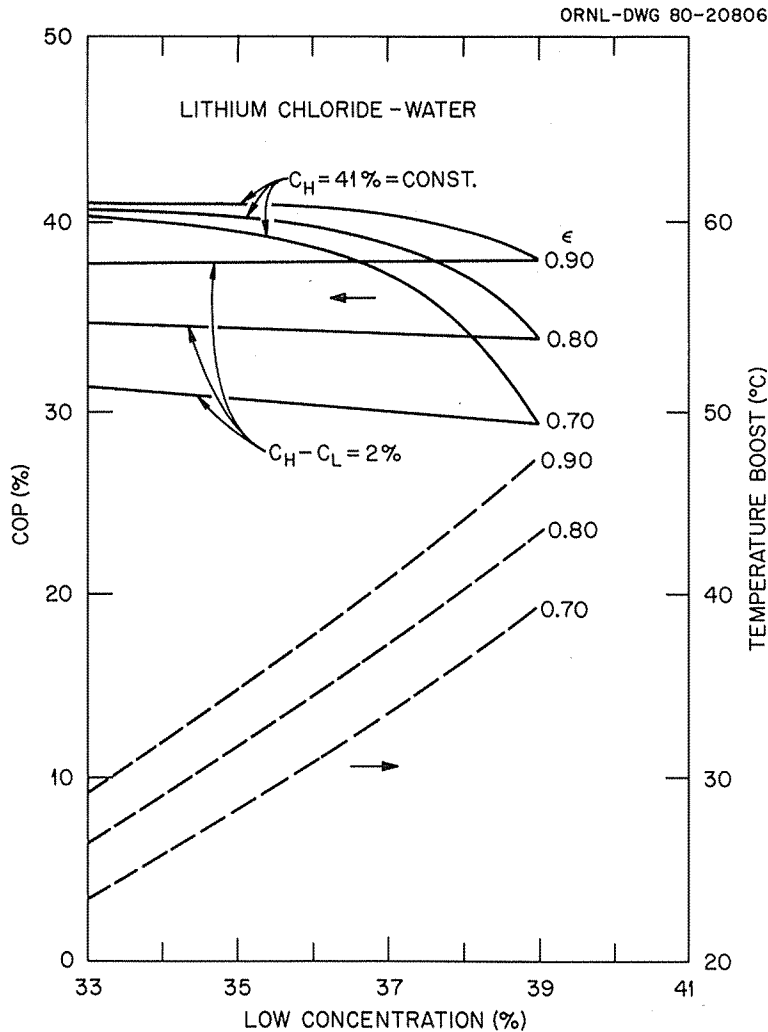


Fig. 21. Performance map showing the effect of concentration on COP and temperature boost for a LiCl-water solution for the two-stage absorption heat pump with a closed desorber.

Figure 22 shows the effect of the waste heat temperature and cooling water temperature on the performance of the heat pump. The COP is plotted as a function of the temperature boost for different values of the above temperatures, and the trade-off between these two performance criteria is evident. The working fluid here is LiBr-water and the effectiveness of all heat exchangers is 0.85. The condensing temperature is assumed to be 5°C higher than the cooling water temperature; similarly, the high solution temperature in the desorber is 5°C lower than the waste heat temperature. It is clear from the figure how raising the waste heat temperature increases performance and raising the cooling water temperature reduces it. Trading off a lower temperature boost against a higher COP is achieved by reducing the low concentration. There is a limit to that, as the COP reaches an asymptotic value of about 40%. The theoretical COP obtainable with a Carnot heat pump, operating with 60°C waste heat and 15°C cooling water, is shown for

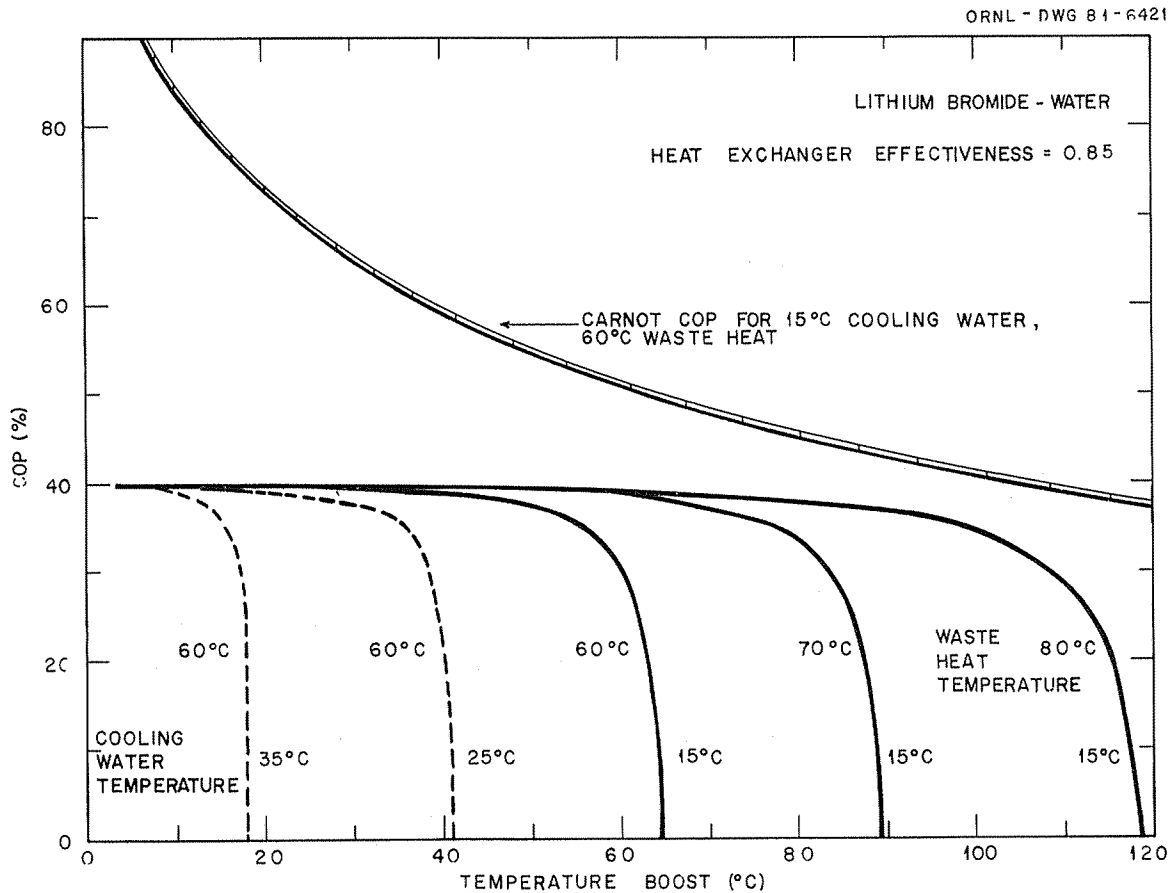


Fig. 22. General performance map showing the effect of various heat source and heat sink temperatures for the two-stage closed-cycle heat pump.

comparison with the corresponding absorption heat pump curve. Figure 22 may be regarded as a summary of all previous calculations, describing the overall system performance for different operating conditions.

Figure 23 shows the COP and delivery temperature vs the desorber approach temperature for a LiBr-water open cycle (see Fig. 9). The effectiveness of all heat exchangers was varied from 0.7 to 0.9. The vapor pressures in both absorbers were chosen so as to flash-evaporate about 1% of the water entering the evaporators in all cases. The inlet air conditions are 32°C and 50% relative humidity, the inlet water temperature is 60°C, and a 2% concentration change in the desorber was assumed.

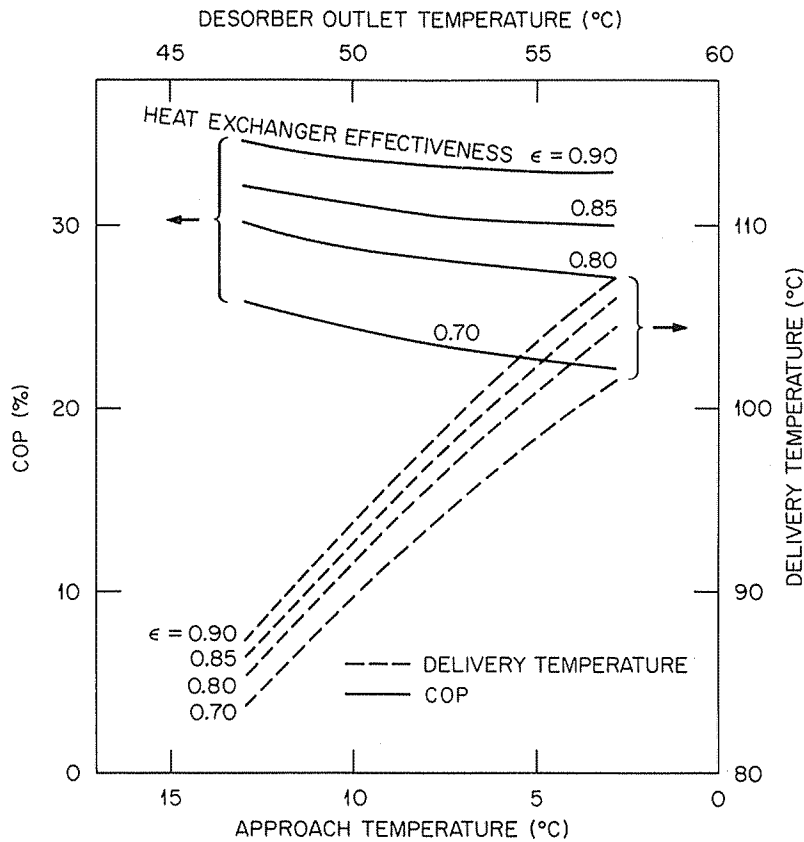


Fig. 23. Performance map showing the effect of approach temperature on delivery temperature and COP for a LiBr-water solution for the two-stage absorption heat pump with an open desorber.

It is seen that the COP depends weakly on the approach temperature and rather strongly on the effectiveness of the heat exchangers. Conversely, the delivery temperature changes quite rapidly with the approach temperature and slowly with the effectiveness. This point is illustrated by noting that for a 3°C approach, an increase in effectiveness from 0.7 to 0.9 increases the COP by about 45%, whereas the delivery temperature is increased by 5% only. Thus, in order to maximize the temperature boost, it is desirable to design the desorber for small approach temperatures. This design will tend to increase the capital costs, because large exchange areas will be needed. On the other hand, if a large COP is not called for, the effectiveness of the heat exchangers may be reduced without affecting the delivery temperature by much. This reduction tends, in turn, to reduce capital costs.

The overall performance chart for a LiCl-water cycle is depicted in Fig. 24. The same desorber vapor pressure was used for both Figs. 23 and 24, and the same trends can be seen. Note that for equivalent desorber conditions and heat exchanger effectiveness, the delivery temperature for a LiBr cycle is 2 to 3°C above that of a LiCl cycle.

Figures 23 and 24 show the effect of the approach temperature on cycle performance for a given concentration change (2%). The effect of increasing concentration changes on the COP and temperature boost is shown in Fig. 25 for various waste heat temperatures and for a fixed approach temperature. For example, for a waste heat temperature of 60°C, the maximum temperature boost (45°C) takes place for a COP equal to zero. As the concentration change increases, so does the COP, and the temperature boost decreases.

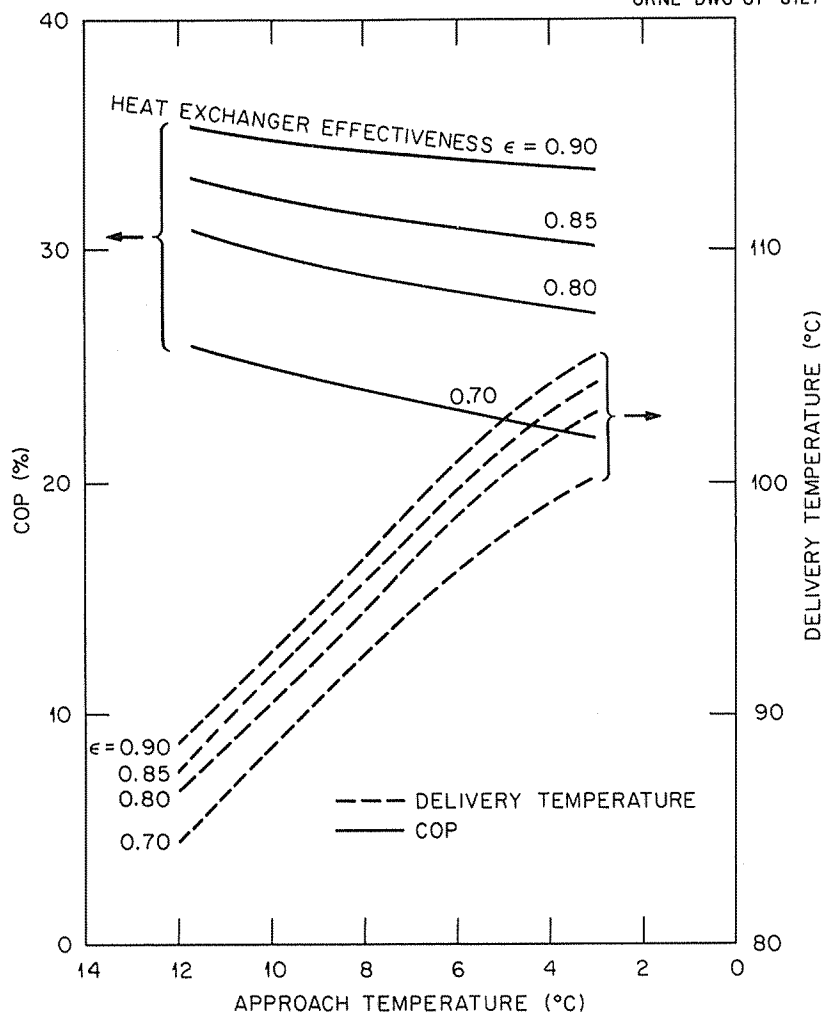


Fig. 24. Performance map showing the effect of approach temperature on delivery temperature and COP for a LiCl-water solution for the two-stage absorption heat pump with an open desorber.

When the concentration change is large, practically no heat may be recovered in the intermediate recuperators. At this point, the COP tends to level off.

Changes in the atmospheric air conditions greatly influence the output temperatures. Figure 26 displays this temperature boost for LiBr and LiCl solutions vs the wet-bulb temperature. Low wet-bulb temperatures mean reduced water vapor pressures in the air and increased brine concentrations in the cycle, which bring about large temperature boosts. For high wet-bulb temperatures, the temperature boosts decrease. To preserve their magnitude, it becomes necessary to increase the amount of air circulated for a given concentration change. Increasing the amount of air circulated decreases the water vapor pressure in the air at the desorber outlet, thus allowing for larger brine concentrations. The parasitic power for air circulation is, however, increased too.

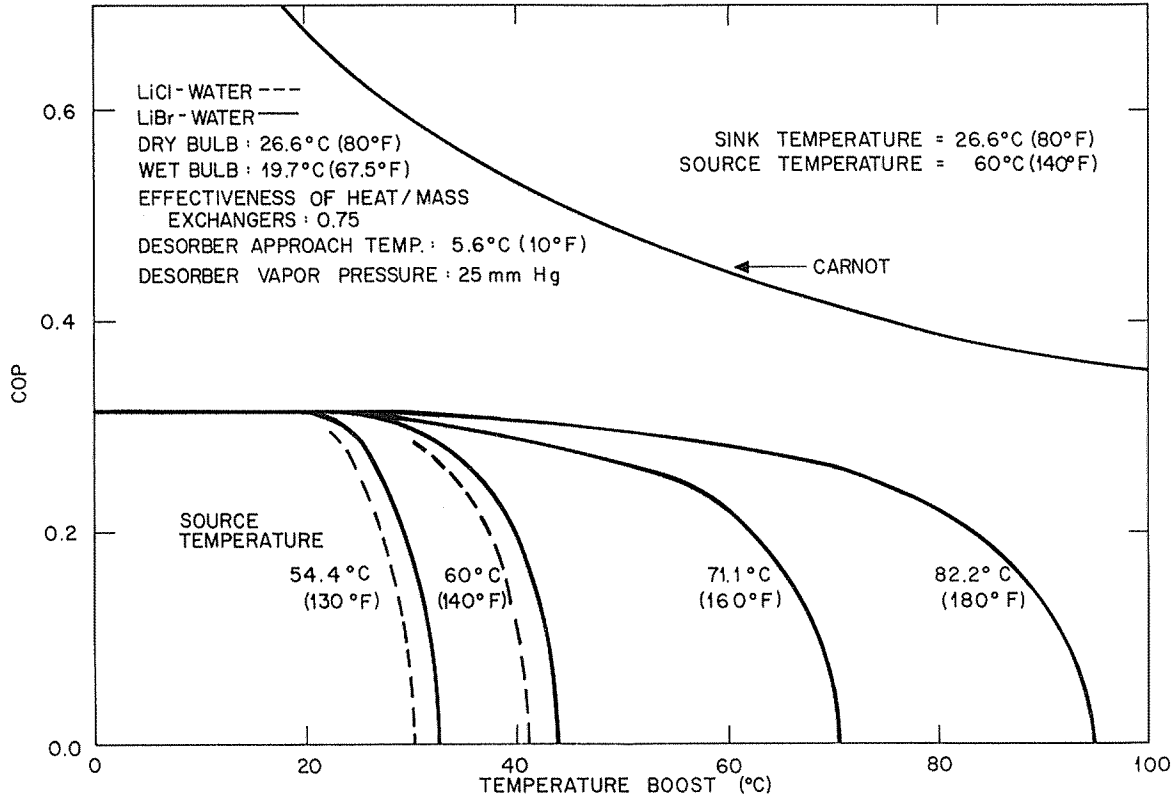


Fig. 25. General performance map showing the effect of different heat source temperatures for the two-stage open-cycle heat pump.

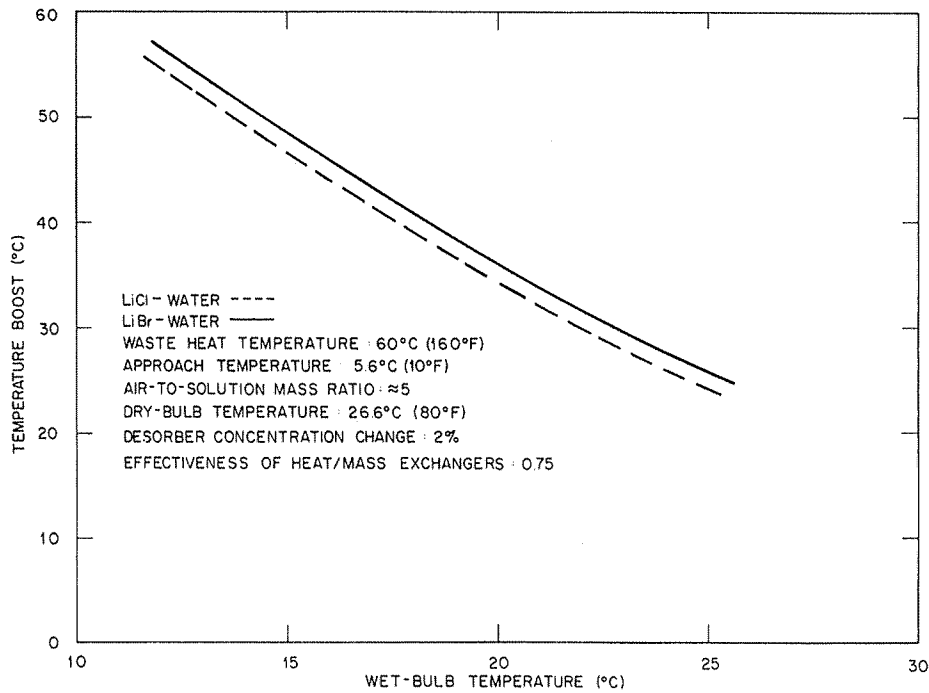


Fig. 26. Influence of the air wet-bulb temperature on the temperature boost for an open-cycle heat pump.

## 8. CONCLUSIONS

A thermodynamic analysis of an absorption heat pump cycle has been performed. The system operates on low-grade heat, without large inputs of electrical energy or of high-temperature heat. This feature alone makes it extremely attractive from the standpoint of energy conservation. The actual design of the system should attempt to minimize the parasitic power required for operation. Two working materials, LiBr-water and LiCl-water, have been considered, and the performance was analyzed in both closed- and open-cycle configurations.

The combination LiBr-water offers the important advantage over LiCl-water of achieving a higher temperature boost. This consideration alone may make LiBr solutions the preferred working fluid, at least for closed cycles. However, LiCl solutions are less corrosive and more stable than LiBr solutions in the presence of air. Thus, they should be seriously considered for open-cycle implementation, in spite of their inferior thermodynamic suitability.

The analysis of the absorber/evaporator system, common to both the open and closed cycles, shows that, to maximize the temperature boost, it is necessary to operate at high concentrations ( $C_H$ ) with a relatively small concentration change ( $C_H - C_L$ ). A small concentration change, however, may be undesirable as it tends to decrease the COP. In an actual design, it becomes necessary to trade off a high temperature boost for a lower heat gain. The absorber performance maps presented in this report are a useful guide in selecting practical operational conditions that can be met without increasing the parasitic power requirements beyond reasonable limits.

The analysis of the closed-cycle desorber shows that the higher the cooling water temperature, the larger the flow rates of both cooling and waste hot water required to produce a given change in concentration. The most favorable operational conditions from the point of view of reduced flow rates take place when relatively cold cooling water is available. A maximum heat sink temperature exists for each given waste heat temperature, above which the system cannot perform.

If the cooling water temperature is relatively close to the waste heat temperature, it is still possible to recover the waste heat by means of an open desorber. The analysis of this device shows that low approach temperatures are desirable in the desorber in order to reduce the amount of air handled, and, consequently, the parasitic power required. An air-to-air heat recuperator must usually be added to an open desorber for good cycle efficiency. The installation of this recuperator, however, increases capital costs. Thus, this recuperator may be desirable only in those instances where the user will be paying for the waste heat rather than receiving a credit for its disposal. Open desorbers/recuperators may operate very efficiently, especially on cold winter days when both sensible and latent heat may be recovered in the recuperator.

The overall system analysis for both closed and open cycles confirms and expands the conclusions extracted from the component analysis: A large temperature boost calls for large values of the maximum cycle concentration and for small concentration changes. For increasing concentration changes, the temperature boost is decreased, but the thermal COP increases. Also, the effectiveness of the heat exchangers has a greater influence on the thermal COP than on the temperature boost. This is a favorable circumstance because the size of the heat exchangers may then be reduced. Although efficiency will decrease, a large temperature boost will be maintained.

The overall conclusion of this report is that absorption cycles offer a good opportunity to recover waste heat for temperature boosting applications. The development of closed-cycle machines calls for knowledge and technology as presently required for the design and construction of absorption chillers. Open-cycle absorption heat pumps are a step beyond closed cycles in terms of development needs: The design of efficient open desorbers and continuous purge systems should be addressed before attempting to implement open cycles.

Previous work in the field of waste heat utilization, carried out at Oak Ridge National Laboratory [3], indicated that absorption cycles have good potential applications for enhancing energy conservation via heat recovery. As such, they were identified as an appropriate subject for research and development. Within that framework, the findings of this report indicate that the development of absorption heat pumps for waste heat recovery is both feasible and desirable, as temperature boosts of about 45°C with COPs of 30% may be realized. Thus, research and development efforts focused on closed systems and on open desorbers are the next reasonable steps for implementing absorption heat pumps.

## Appendix

### OPEN DESORBER PERFORMANCE CALCULATIONS

The heat and mass transfer processes taking place in the open desorber are analyzed here. As stated before, it is assumed that the solution vapor pressure is maintained constant during desorption and that the resistance to mass transfer is concentrated on the air side of the air-solution interface.

The differential of water mass  $dm_w$  exchanged per unit time between the solution surface with a vapor pressure  $p_s$  corresponding to a humidity ratio  $W_i$  and an air stream with humidity ratio  $W$  may be written as [26]:

$$dm_w = h_D(W_i - W) da_i , \quad (\text{a.1})$$

with

$$W_i = 0.622P_s/(P - P_s) ,$$

where  $h_D$  is the mass transfer coefficient,  $da_i$  is the differential of the interface area, and  $P$  is the total air pressure. The change of humidity ratio  $dW$  for the air stream of mass flux  $m_a$  is

$$m_a dW = dm_w . \quad (\text{a.2})$$

From Eqs. (a.1) and (a.2), one obtains

$$m_a dW = h_D(W_i - W) da_i . \quad (\text{a.3})$$

Similarly, a thermal balance for the air phase yields

$$m_a dh_a = h(T_i - T) da_i + m_a h_i dw , \quad (\text{a.4})$$

where  $h_a$  is the enthalpy of humid air, dependent both on its temperature and humidity,  $T$  is the air temperature,  $h$  is the heat transfer coefficient from the interface to the air,  $T_i$  is the interface temperature, and  $h_i$  is the enthalpy of the water vapor evolved from the solution interface. The above enthalpies may be expressed as follows:

$$h_a = C_{pa}T + W(h_{fg_0} + C_{pw}T) , \quad (\text{a.5})$$

$$h_i = h_{fg_0} + C_{pw}T , \quad (\text{a.6})$$

where  $C_{pa}$  and  $C_{pw}$  are the specific heats of dry air and water, respectively, and  $h_{fg_0}$  is the latent heat of vaporization of water at 0°C (32°F). Combining Eqs. (a.3) and (a.4) and using Eqs. (a.5) and (a.6), one obtains

$$\frac{dT}{T_i - T} = \frac{h}{C_p h_D} \times \frac{1}{W_i - W} + \frac{C_{pw}}{C_p} dW, \quad (\text{a.7})$$

where  $C_p = C_{pa} + WC_{pw}$  is the specific heat of humid air.

The ratio  $(h/h_D C_p)^{3/2}$  is the Lewis number, which for turbulent transport of water vapor in air is given by [27]:

$$(h/h_D C_p)^{3/2} = D/\alpha, \quad (\text{a.8})$$

where  $\alpha = k/\rho c_p$ , with  $k$  = thermal conductivity of air,  $c_p$  = specific heat of air,  $\rho$  = air density, and  $D$  = diffusivity of water vapor in air. As shown in [27], the Lewis number is close to one. Since  $C_{pw}/C_p$  is of order unity and  $W_i - W$  is generally small (about  $10^{-2}$ ), Eq. (a.7) may be approximated as:

$$dT = [(T_i - T)/(W_i - W)] \cdot dW. \quad (\text{a.9})$$

Integration of this equation for constant  $T_i$  yields the air temperature change along the desorber:

$$\ln \frac{W_i - W_{22}}{W_i - W_{27}} \approx \int_{22}^{27} \frac{dT}{T_i - T}. \quad (\text{a.10})$$

Rigorously,  $T_i$  (the interface temperature) should be taken as the temperature distribution corresponding to a constant solution vapor pressure. For small concentration changes in the desorber (in the order of 2%), however,  $T_i$  does not vary more than 4°C. Thus, by assuming  $T_i$  constant and equal to the exit solution temperature  $T_{26}$ , it is possible to obtain:

$$\frac{W_i - W_{22}}{W_i - W_{27}} \approx \frac{T_i - T_{22}}{T_i - T_{27}}, \quad (\text{a.11})$$

which relates the air humidity changes to the air temperature changes in the desorber. Equation (a.11) provides a relation between the change in air humidity and the corresponding change in the air temperature. This equation is listed as Eq. 40 in Chap. 6. For large concentration changes, the following equation was used:

$$T_{27} - T_{22} = \int_{W_{22}}^{W_{27}} \frac{T_i - T}{W_i - W} dW. \quad (\text{a.12})$$

## REFERENCES

1. J. Blue and J. Arehart, *A Pocket Reference of Energy Facts and Figures*, Oak Ridge National Laboratory, Oak Ridge, Tenn., October 1979.
2. M. H. Chiogioji, *Industrial Energy Conservation*, Marcel Dekker, Inc., New York, 1979.
3. H. Perez-Blanco, *Heat Pump Concepts for Industrial Use of Waste Heat*, ORNL/TM-7655 (1981).
4. D. A. Reay, *Industrial Energy Conservation*, Pergamon Press, Oxford, 1977.
5. N. Isshiki, "Study on the Concentration Difference Energy System," *J. Non-Equilib. Thermodynamics* 2: 85-107 (1977).
6. I. Shwarts and A. Shitzer, "Solar Absorption System for Space Cooling and Heating," *ASHRAE J.*, November 1977, 51-54.
7. K. F. Knoche and D. Stetmeier, "Absorption Heat Pumps for Solar Space Heating Systems," *Studies in Heat Transfer*, Hemisphere Publishing Corp., Washington, 1979.
8. K. L. Sauer, "Absorption Type Heat Pump," *Sonnenenergie Waermepumpe* 4(2/3): 15-19 (1979).
9. "Heat Transformer Makes Waste Heat Efficient Source," *Des. News*, Oct. 22, 1979.
10. G. Cohen, J. Salvat, and A. Rojey, "A New Absorption-Cycle Process for Upgrading Waste Heat," *Proceedings of the 14th Intersociety Energy Conversion Engineering Conference*, Boston, Mass., Aug. 5-10, 1979, vol. 2, pp. 1720-24.
11. H. Perez-Blanco and F. Chen, "Some Heat Pump Concepts for Residual Heat Utilization," *Third Miami International Conference on Alternative Energy Sources*, Miami Beach, Fla., Dec. 15-17, 1980.
12. D. A. Williams and J. B. Tiedemann, "A Heat Pump Powered by Natural Thermal Gradients," *Proceedings of the 9th Intersociety Energy Conversion Engineering Conference*, Aug. 26-30, 1974, pp. 538-40.
13. R. Best, "Methanol-Lithium Bromide, Zinc Bromide Mixture Applied to Solar Absorption Heat Pumps," *Proceedings of the International Conference on Solar Building Technology*, London, England, July 25, 1977, vol. 2, pp. 437-43.
14. E. C. Clark and C. C. Hiller, "Development and Testing of the Sulfuric Acid-Water Chemical Heat Pump/Chemical Energy Storage System," *Proceedings of the 14th Intersociety Energy Conversion Engineering Conference*, Boston, Mass., Aug. 5-10, 1979, vol. 1, pp. 510-15.
15. P. Offenhartz and F. Brown, "Methanol-Based Heat Pumps for Storage of Solar Thermal Energy," *Proceedings of the 14th Intersociety Energy Conversion Engineering Conference*, Boston, Mass., Aug. 5-10, 1979, vol. 1, pp. 507-9.

16. H. M. Factor and G. Grossman, "A Packed Bed Dehumidifier/Regenerator for Solar Air Conditioning with Liquid Dessicants," *Sol. Energy* **24**: 541-50 (1980).
17. R. K. Collier, "The Analysis and Simulation of an Open-Cycle Absorption Refrigeration System," *Sol. Energy* **23**: 357-66 (1979).
18. R. M. Buffington, "Qualitative Requirements for Absorbent-Refrigerant Combinations," *Refrig. Eng.* **57**: 343 (1949).
19. W. R. Hainsworth, "Refrigerants and Absorbents," *Refrig. Eng.* **48**: 97 (1944).
20. P. J. Wilbur and S. Karaki, *Solar Cooling*, The Franklin Institute Press, Philadelphia, 1977.
21. G. Grossman and I. Shwarts, "An Open Absorption System for Solar Air Conditioning," *Proceedings, the Conference on Heat Transfer in Buildings*, Dubrovnik, Yugoslavia, August-September 1977, vol. 2, pp. 641-47.
22. L. A. McNeely, "Thermodynamic Properties of Aqueous Solutions of Lithium Bromide," *ASHRAE Trans.* **85**: 413 (1979).
23. F. R. Bichowsky, "Chemical Dehumidification Agents," *Heat., Piping, Air Cond.* **12**: 627 (1940).
24. H. F. Gibbard and G. Scatchard, "Liquid-Vapor Equilibrium of Aqueous Lithium Chloride," *J. Chem. Eng. Data* **18**: 293-98 (1973).
25. W. M. Kays and A. L. London, *Compact Heat Exchangers*, McGraw Hill, New York, 1964.
26. *ASHRAE Handbook and Product Directory*, 1979 equipment volume.
27. J. L. Threlkeld, *Thermal Environmental Engineering*, Prentice Hall, Englewood Cliffs, N. J., 1970.

## INTERNAL DISTRIBUTION

- |                       |                                  |
|-----------------------|----------------------------------|
| 1. R. W. Barnes       | 27. L. N. McCold                 |
| 2. W. F. Barron       | 28. V. C. Mei                    |
| 3. V. D. Baxter       | 29. J. W. Michel                 |
| 4. F. C. Chen         | 30. W. R. Mixon                  |
| 5. W. L. Cooper, Jr.  | 31. C. L. Nichols                |
| 6. F. A. Creswick     | 32. F. S. Patton                 |
| 7. G. A. Dailey       | 33-37. H. Perez-Blanco           |
| 8. R. C. DeVault      | 38. A. M. Perry                  |
| 9. J. E. Dobson       | 39. R. C. Robertson              |
| 10. R. D. Ellison     | 40. G. Samuels                   |
| 11. F. D. Fairchild   | 41. A. D. Shepherd               |
| 12. S. K. Fischer     | 42. R. C. Tepel                  |
| 13. W. Fulkerson      | 43. L. F. Truett                 |
| 14-18. G. Grossman    | 44. T. A. Vineyard               |
| 19. G. R. Hadder      | 45. R. L. Wendt                  |
| 20. V. O. Haynes      | 46. T. Wilbanks                  |
| 21. K. E. Heidenreich | 47. Emergency Technology Library |
| 22. G. E. Kamp        | 48-50. Laboratory Records Dept.  |
| 23. S. I. Kaplan      | 51. Laboratory Records—RC        |
| 24. M. A. Karnitz     | 52. ORNL Patent Office           |
| 25. J. O. Kolb        | 53-54. Central Research Library  |
| 26. C. G. Lawson      | 55. Document Reference Section   |

## EXTERNAL DISTRIBUTION

56. Ing. Jacob Agrest, Unigueletes 1100, Buenos Aires, Argentina
57. Prof. George Alefeld, Physik-Department E 10, der Technischen Universität München, D-8046 Garching, Fed. Rep. Germany
58. Donald A. Allen, Dept. of Agriculture and Rural Development, Florenceville, RR 2, New Brunswick, EOJ 1KO Canada
59. Redfield W. Allen, University of Maryland, Mechanical Engineering Dept., College Park, MD 20742
60. Fred W. Bawel, Arkla Industries, Inc., 810 E. Franklin Street, P.O. Box 534, Evansville, IN 47701
61. Jonathan Ben-Dror, Tadiran ASD, P.O. Box 648, Tel-Aviv, Israel
62. J. Berghmans, M.S., Ph.D., Katholieke Universiteit Leuven, Instituut Mechanica, Celestijnenlaan 300 A, B-3030 Heverlee-Belgium
63. Dr. Wendell Bierman, Carrier Corporation, Summit Landing, P.O. Box 4895, Syracuse, NY 13221
64. Joseph R. Bourne, P.O. Box 17144, Tucson, AZ 85731
65. Charles E. Bullock, Research Division, Carrier Corporation, P.O. Box 4808, Carrier Parkway, Syracuse, NY 13221
66. James M. Calm, Energy and Environmental Systems Division, Argonne National Laboratory, Argonne, IL 60439
67. E. C. Clark, Rocket Research Company, York Center, Redmond, WA 90852
68. Ing. Herman K. A. De Lange, Industrie Riunite Eurodomestici, 21025 Comerio, Varese, Italy
69. Dr. David Didion, National Bureau of Standards, Bldg. 226, Washington, DC 20234

70. Richard A. English, Carrier Corporation, Summit Landing, P.O. Box 4895, Syracuse, NY 13221
71. Robert D. Fischer, Battelle Columbus Laboratories, 505 King Avenue, Columbus, OH 43201
72. Dr. William T. Hanna, Battelle Columbus Laboratories, 505 King Avenue, Columbus, OH 43201
73. Dr. Bruce Hannon, University of Illinois, 128 Observatory Blvd., Urbana, IL 61801
74. Floyd Hayes, Bldg. 12-G, The Trane Company, 3600 Thomas Creek Road, La Crosse, WI 54601
75. Prof. J. Howell, Dept. of Mechanical Engineering, The University of Texas at Austin, Austin, TX 78712
76. Wallace Johnson, Concentration Specialists, Inc., 26 Dundee Park, Andover, MA 01810
77. P. Joyner, Vice President—Research, The Trane Company, 3600 Thomas Creek Road, La Crosse, WI 54601
78. James Kamm, 2022 Adams Street, Toledo, OH 43634
79. Prof. Zalman Lavan, Dept. of Mechanical Engineering, Illinois Institute of Technology, Chicago, IL 60616
80. Harold E. Loewer, Reinhold-Schneider, STR 135, 75 Karlsruhe 51, Germany
81. Dr. Harold Lorsch, Franklin Research Center, Philadelphia, PA 19103
82. Lowell A. McNeely, 7310 Stenmeier Drive, Indianapolis, IN 46250
83. Richard Merrick, Arkla Industries, Inc., P.O. Box 534, Evansville, IN 47704
84. Donald K. Miller, York Div. of Borg Warner Corp., Grantley Road, York, PA 17403
85. Benjamin A. Phillips, Phillips Engineering Co., 721 Pleasant Street, St. Joseph, MI 49085
86. James M. Porter, The Trane Company, 3600 Pammel Creek Road, La Crosse, WI 54601
87. Dr. Wiktor Radlow, Dept. of Physical Chemistry, The Royal Institute of Technology, Stockholm, Sweden
88. Odd Sangesland, Grumman Aerospace Corporation, Bldg. B30-30, Bethpage, NY 11714
89. Raymond F. Stevens, Hartford Steam, Boiler Inspection and Ins. Co., 56 Prospect Street, Hartford, CN 06102
90. C. J. Swet, 7040 Woodville Road, Mt. Airy, MD 21771
91. Prof. Gary C. Vliet, Dept. of Mechanical Engineering, The University of Texas at Austin, Austin, TX 78712
92. Dr. Michael Wahlig, Lawrence Berkeley Laboratory, Berkeley, CA 94720
93. Prof. Gunnar Wettermark, Dept. of Physical Chemistry, The Royal Institute of Technology, Stockholm, Sweden
94. Eugene P. Whitlow, 1851 N. Valley View Drive, St. Joseph, MI 49085
95. Office of the Assistant Manager for Energy Research and Development, U.S. Department of Energy, Oak Ridge Operations, Oak Ridge, TN 37830
- 96-122. Technical Information Center, Department of Energy, P.O. Box 62, Oak Ridge, TN 37830
- 123-272. Energy Division Library, Oak Ridge National Laboratory, P.O. Box Y, Bldg. 9102-2, Room 218, Oak Ridge, TN 37830